Neuroprotective compound Quercetin from endophytic fungus, *Nigrospora oryzae* isolated from *Tinospora cordifolia*

A Dissertation submitted in partial fulfillment of the requirement for the award of degree of

Master of Technology

In

Biotechnology

Submitted by

Rajat Vig

Roll No.: 601704003

Under the guidance of

Dr. M Vasundhara

Assistant Professor

DEPARTMENT OF BIOTECHNOLOGY

THAPAR INSTITUTE OF ENGINEERING & TECHNOLOGY

PATIALA-147004

July 2019

DECLARATION

I, hereby declare that the work done in this project entitled, "Neuroprotective compound Quercetin from endophytic fungus, *Nigrospora oryzae* isolated from *Tinospora cordifolia*" submitted towards partial fulfillment of requirement for the award of **Master of Technology** in Biotechnology, Department of Biotechnology, Thapar Institute of Engineering and Technology, Patiala, is an authentic record of the work carried out by me under the supervision and guidance of **Dr. M Vasundhara, Assistant Professor Department of Biotechnology, Thapar Institute of Engineering and Technology, Patiala.**

The matter embodied in this report has not been submitted in part or full to any other University or institute for the award of any degree.

Rajat

Rajat Vig

Roll No. 601704003

M.Tech. (Biotechnology)

Date: 17/08/2019

Place: Patiala

CERTIFICATE

This is to certify that the dissertation entitled "Neuroprotective compound Quercetin from endophytic fungus, *Nigrospora oryzae* isolated from *Tinospora cordifolia*" submitted for the degree of Master of Technology in the subject of Biotechnology at Thapar Institute of Engineering and Technology (TIET), Patiala is a bonafide work carried out by **Mr. Rajat Vig** under my supervision and guidance.

To the best of my knowledge, the matter embodied in this dissertation has not been submitted to any other university/institute for the award of any Degree or Diploma.

Vasundhara

Dr. M Vasundhara

Assistant Professor

Department of Biotechnology

Thapar Institute of Engineering and Technology, Patiala

Acknowledgements

I want to express my deepest gratitude and sincere thanks to the following people without whom my thesis could not have been possible. I thank the almighty for his blessings in the completion of the project.

First and foremost, I am sincerely grateful from the bottom of my heart to my supervisor and guide, **Dr. M Vasundhara** for her continuous support, trust, motivation, patience, enthusiasm and knowledge which helped me to successfully carry out this project. I am thankful to her for resolving every problem, guidance and friendly advice in every phase of the project which helped in shaping this thesis perfectly.

I am deeply thankful to **Dr. Anil Kumar** (Head of TIFAC-CORE) and **Dr. MS Reddy**, Associate Dean, Thapar Institute of Engineering and Technology for providing me with all the lab instruments and facilities required in TIFAC CORE

I express my thanks to **Dr. Sairam Krishnamurthy**, Professor, Department of Pharmaceutical Engineering and Technology, Indian Institute of Technology (B.H.U.) for helping me in carrying out *in vivo* analysis.

I would like to thanks **Dr. Moushumi Ghosh**, Professor and Head, Department of Biotechnology, for providing with the best laboratory facilities.

I express my deepest thanks to **Ms. Tanveer Kaur, Ms. Fatima and Ms. Anu Gupta** who despite of her completion of project, was constantly resolving all my doubts and encouraging me at every step.

I was fortunate enough to avail help and assistance from laboratory staff, **Mr. Soni, Mr. Ram Nawal, Mr. Lallan and Mr. Surinder**.

I would like to thanks **SAIF labs, Punjab University, Chandigarh** for extending their facilities for characterization.

A special thanks to my **family** and my M.Tech. friend **Naina Saini** for their direct or indirect motivation throughout the project.

TABLE OF CONTENTS

List of Figures

List of Tables

Abbreviations

µg	Microgram
AA	Ascorbic acid
Ach	Acetylcholine
AChE	Acetylcholinesterase
AD	Alzheimer's disease
ATCI	Acetylthiocholine iodide
ChAT	Choline acetyltransferase
DPPH	2,2-diphenyl-1-picryl-hydrazyl
DPZ	Donepezil
DTNB	5,5'-dithiobis(2-nitrobenzoic acid)
ESI-MS	Electrospray ionization mass spectrometry
FTIR	Fourier transform infrared spectroscopy
GL	Giloy leaf
LPO	Lipid peroxidation
Mg	Milligram
Ml	Millilitre
^{o}C	Degree centigrade
PAT	Passive avoidance test
PDA	Potato dextrose agar
PDB	Potato dextrose broth
SCO	Scopolamine
TLC	Thin layer chromatography
UV	Ultraviolet

Abstract

Alzheimer's disease (AD) is considered as one of the most prevalent neurodegenerative disorder. Dementia is one of the core symptom of AD. *Tinospora cordifolia* exhibits neuroprotective activity. Moreover, endophytic mycobiota of *Tinospora cordifolia* possesses antigout, anticancer and antioxidant properties. Therefore, the present study investigated the therapeutic effects of endophytic fungi obtained from medicinal plant, *Tinospora cordifolia* in an experimental animal model of dementia. *In vitro* acetylcholinesterase (AChE) inhibitory and anti-oxidant assays revealed that GL15 showed significant effect which was equivalent to reference drugs. GL15 (5 mg/kg; i.p.) attenuated the SCO-induced loss in spatial recognition memory in Y-maze and PAT. The SCO-induced modulation in cholinergic pathway was ameliorated by GL15 (5 mg/kg) in hippocampus, resulting in decrease in acetylcholinesterase activity. GL15 (5 mg/kg) restored the cytoarchitecture of hippocampus. Subsequently, the effect of GL15 (5 mg/kg) on AChE-mediated mechanism in pathophysiological condition of dementia was evaluated. GL15 (5 mg/kg) showed the significant decrease in expression of AChE activity. These results were comparable with donepezil. These observations emphasize the fact GL15 may show improvement in cognitive impairments in animals through AChE-mediated mechanism. GL15 could be a potential therapeutic option in the management of AD. Column chromatography was run to obtain various fractions of GL15 and fraction 3 of GL15 showed 87.1% percentage AChE inhibition. UV absorbance of fraction 3 of GL15 was identical to that of quercetin. In FTIR of fraction 3, percentage transmittance vs wave numbers showed spectrum which was analogous to quercetin. Positive ionization mode of ESI-MS showed the m/z value of 303.22 which was similar to that of quercetin. Based upon the various techniques of characterization, it may be concluded that quercetin is present in fraction 3 of GL15. Endophytic fungus GL15 was identified through microscopic and molecular techniques and it was observed that GL15 showed showed septate hyphae and spore morphology similar to *Nigrospora oryzae*. Molecular identification confirmed that GL15 was *N. oryzae* as phylogenetic tree showed clustering of GL15 with *Nigrospora oryzae.*

Chapter 1 Introduction

Alzheimer's disease is considered as the key epidemic among neurodegenerative disorders with the pervasiveness persisting to increase in part because of the old age world population (Weller et al., 2018; Pilipenko et al., 2019). Dementia is a hallmark symptom of Alzheimer's disease in the old age people that ensues in loss of their independence which leads to reliance on other individuals or caretakers. Additionally, remarkable emotional and financial burden on the society arises (Cai et al., 2018). Current preclinical and clinical pathophysiological studies suggest that amelioration of cholinergic pathway in Alzheimer's disease-like dementia helps in recovery of cognitive deficits (Fig. 1) (Kim et al., 2018). Moreover, decrease in the level of acetylcholine (ACh) leads to cognitive deficits (Sun et al., 2019).

Literature review demonstrated that scopolamine is a well established muscarinic receptor antagonist for the assessment of cognitive anomalies in preclinical studies. Further, cholinergic attenuation and impairments in cognition occur due to administration of scopolamine in amnesic mice (Shabani et al., 2018). Till date, several synthetic acetylcholinesterase inhibitors like donepezil and galantamine are permitted by FDA in the management of gentle dementia but their use is limited due to minute therapeutic accomplishment and various side effects (Mushtaq et al., 2018; Choi et al., 2018). Therefore, it is required to investigate novel drugs which may exhibit therapeutic effects against dementia.

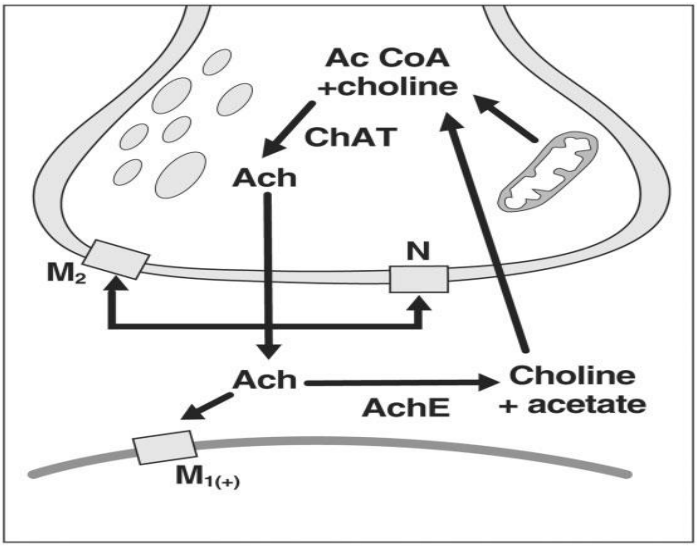

Fig. 1 Cholinergic pathway (Hampel et al., 2018)

Acetylcholine is released from pre-synaptic vesicles of cholinergic neurons through choline acetyltrasferase (ChAT). Acetylcholinesterase (AchE) breaks down acetylcholine (Ach) into choline and acetic acid. 5,5'-dithiobis-(2-nitrobenzoic acid) (DTNB) binds with choline to produce yellow color during acetylcholinesterase inhibitory activity. Choline is recycled back to pre-synaptic vesicle and binds with acetyl coenzyme A (Ac CoA) to form acetylcholine. Acetyl coenzyme A is released from mitochondria.

Bioactive compounds isolated from endophytic fungi are well known for their therapeutic properties, so these can be considered as a possible remedial alternative option in the attenuation of scopolamine-induced dementia (Tewari et al., 2018; Ohno et al., 2018; Kim et al., 2018; Bhattacharjee et al., 2015). *Tinospora cordifolia* frequently recognized as Guduchi is a climbing shrub found chiefly in humid parts of India and China (Mishra et al., 2012). Ethnopharmacological studies suggest that *Tinospora cordifolia* possesses anti-androgenic, anti-inflammatory and anxiolytic properties in addition to cognitive anomalies amelioration (Dhama et al., 2016; Mishra et al., 2015; Rajalakshmi et al., 2016; Singh et al., 2016; Mishra et al., 2013). Furthermore, recently (Kosaraju et al., 2014) has reported that *Tinospora cordifolia* shows anti-Parkinson effects in 6-hydroxy dopamine rat model. *Tinospora cordifolia* has a broad range of antioxidants. *Tinospora cordifolia* has shown significant antioxidant activity *in vitro* (Mushtaq et al., 2018). In preclinical studies *Tinospora cordifolia* significantly decreased the LPO and raised the concentration of antioxidant enzymes in hippocampus (Rawal et al., 2004).

Endophytes are concealed and mainly uncultivated entities of the microbial world (Kharwar et al., 2011). Scores of authors have illustrated that endophytes have a vital role in the fabrication of new-fangled secondary metabolites which possess inhibitory activities against bacteria, fungus and cancer (Verma et al., 2009). It has been reported that *Taxomyces andreanae* from *Taxus brevifolia* produces Taxol, which is a blockbuster drug in the management of cancer (Stierle et al., 1993). Recently, (Kapoor et al., 2018) reported that endophytic fungus of *Tinospora cordifolia* exhibits anti-gout property. Thus, it is illustrated that endophytic fungi from *Tinospora cordifolia* may put forth neuroprotective activity. The clinical manifestation of dementia is increased levels of acetylcholinesterase (AChE) in the hippocampus (Yang et al., 2015; Qu et al., 2017). It has been well suggested that hippocampus is an integrative element of limbic region of brain which influences the cognitive functions (Malekiyan et al., 2019). The clinical role of

hippocampus cannot be excluded while considering the context of dementia as it is critical for the learning and memory. Neurochemical studies suggest that there is a hyperactivity of cholinergic system in hippocampus in case of dementia. It has been revealed that AChE enzymatic activities are up regulated in the dementia-like condition in hippocampus of experimental mice (Kim et al., 2018). As hippocampus plays a decisive function in the amendment of amount of AChE, it is valuable to intricate the AChE-mediated mechanism in the pathophysiology of dementia condition. Moreover, the cholinergic mediated action of *Tinospora cordifolia* fungal extract is unreported in preclinical and clinical studies.

Objectives

- Isolation and *in vitro* screening of endophytic fungi from *Tinospora cordifolia* for acetylcholinesterase inhibition.
- *In vivo* assessment of isolated endophytic fungal extract for acetylcholinesterase inhibition.
- Fractionation, purification and characterization of endophytic crude fungal extract exhibiting acetylcholinesterase inhibitory activity.
- Molecular and microscopic identification of endophytic fungus producing acetylcholinesterase inhibitor.

Chapter 2 Literature review

2.1. What is dementia?

Dementia is a neural disorder illustrated by progressive turn down in more than one cognitive domain which causes loss of capability to execute instrumental or vital actions of daily life (Weller et al., 2018). Dementia ensues from neurodegenerative offense in brain neurons. Neurodegeneration imparts learning and memory anomalies in addition to modification in communal and behavioral acquiescence. Cholinergic hypothesis illustrates the pathogenesis of dementia, due to which sternness of this disease is joined with neuronal harms in septo-hippocampal cholinergic system linked with cognition (Francis et al., 1999). Authors have demonstrated that global expenditure of care and remedy for dementia was reported to be $604 billion in 2011 and has been escalating annually (Kim et al., 2018). Further, synthetic drugs available in the market have multiple adverse effects. Hence, the need of the hour is to explore novel therapeutic agents which might ameliorate dementia.

2.2. Medicinal plant *Tinospora cordifolia*

Tinospora cordifolia, generally known as Giloe, is a huge, glabrous, deciduous climbing shrub (family Menispermiaceae). *Tinospora cordifolia* is indigenous and dispersed throughout the tropical Indian subcontinent, mounting to the height of 300 m (Mishra et al., 2012). Numerous phytochemicals are obtained from *Tinospora cordifolia* (Fig. 2)

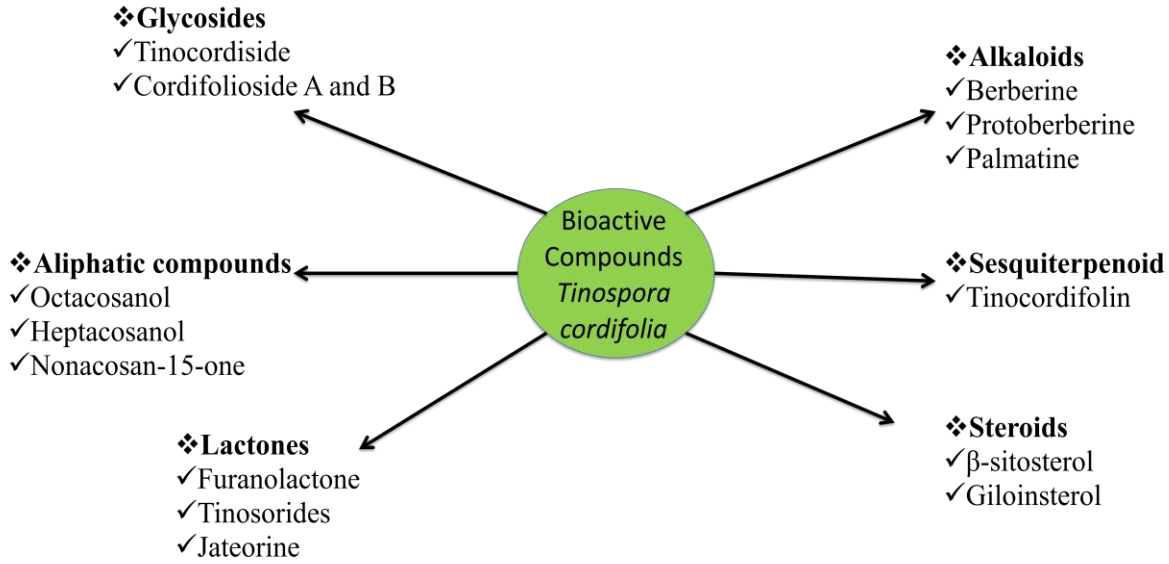

Fig. 2 Bioactive compounds of *Tinospora cordifolia* (Singh et al., 2003).

2.3. Role of *Tinospora cordifolia* in attenuation of various diseases

Tinospora cordifolia ameliorated cadmium-treated significant increase in level of lipid peroxidation (LPO) and decrease in antioxidant activity. In this report, hepatoprotective effects of *Tinospora cordifolia* were revealed against cadmium administered rodents (Baskaran et al., 2018). *Tinospora cordifolia* attenuated cell injury due to oxidative stress in rat hippocampus (Rawal et al., 2004).

Tinospora cordifolia exhibited *in vitro* acetylcholinesterase (AChE) inhibitory property (Vinutha et al., 2007). *Tinospora cordifolia* mitigated glutamate-induced toxicity and might prove beneficial against neurodegeneration (Sharma et al., 2018). Berberine is a phytochemical from *T.cordifolia* has shown neuroprotective activity in animal models (Cicero et al., 2016).

Tinospora cordifolia has shown a crucial role in countering various disorders and possesses neuroprotective, anti-oxidant, anti-hyperglycemic, analgesic, anti-hyperlipidemic, anxiolytic, adaptogenic, antiulcer, anti-inflammatory, anti-cancer, thrombolytic, anti-microbial and anti-diarrheal properties.

Tinospora cordifolia is also a store of micronutrients eg. Cu, Ca, P, Fe, Zn and Mn. In preclinical studies an unusual focus has been made on its health remuneration in curing endocrine and metabolic disorders and its potential as an immune booster. Lots of patents have been filed on bioactive metabolites of *Tinospora cordifolia* which have shown significant therapeutic effects against various diseases and have increased life anticipation of humans (Dhama et al., 2016).

2.4. Endophytic fungi

Endophytic fungi stay inside the plant tissues and have been reported to show prominent mutualistic symbiotic relationships with their host plant (Song et al., 2018). They are prospective sources for a variety of bioactive metabolites with fascinating structures. They possess anti-fungal, antibacterial, antidiabetic, antioxidant and anticancer properties. It is well known that few metabolites may be produced by endophytic fungi living inside the plant (Mishra et al., 2012).

2.5. Endophytic fungi from *Tinospora cordifolia*

1151 endophytic fungi have been obtained from various parts of *Tinospora cordifolia*. Notable organisms like *Aspergillus sydowii, Colletotrichum crassipes* were recognized using

molecular tools. More than 50 percent of the isolated endophytic fungi exhibited antibacterial activity. *C.globosum* and *B rhodina* revealed anti-bacterial effects in opposition to all bacterial species affecting human. However, there was a considerable variation between their activities (Mishra et al., 2012).

In this study, there is stress on the significance of inhibitors of alpha-glucosidase in the pest resistance due to interference of the endophytic fungi. Endophytes have demonstrated a remarkable effect in providing resistance against insect pests. In this report, 34 endophytic fungi of *Tinospora cordifolia* were monitored for their capability to make inhibitors of alpha-glucosidase. *Cladosporium sp*. obtained from *Tinospora cordifolia* exhibited highest percentage of inhibition (Singh et al., 2015).

Isolate of *Cladosporium. Velox* from *T. cordifolia* was extracted with ethylacetate. Total phenol content was found to be 730µg gallic acid equivalent/mL. Extract exhibited antioxidant activity with IC_{50} value of 22.5µg/mL which was analogous to reference control. The phenolic extract revealed significant genoprotective activity in animal model. Evaluation of phenolic components was conceded using RP-HPLC. Mutagenicity and cytotoxicity consequences discovered the extract to be safe and non-toxic in nature (Singh et al., 2016).

Kapoor et al., 2018 have chosen *Tinospora cordifolia* and isolated 19 endophytic fungi to screen for their anti-gout property. In the qualitative test, out of total fungal endophytes, more than one-third endophytic fungi showed more than 30 percent xanthine oxidase inhibition, of which some of the isolates were set up to exhibit xanthine oxidase inhibition in the array of 38-45%.

2.6. Neuroprotective effects of endophytic fungi of various medicinal plant

Bioactive compounds 5-methoxy-2-methyl-3-tricosyl-1,4-benzoquinone and 1-O-methylemodin obtained from endophytic fungus *Colletotrichum* of *Huperzia serrat*a have shown anti-AChE activity (Li et al., 2018).

Colletotrichum sp. was obtained from *Morus alba* universally acknowledged as mulberry. Neuroprotective properties of bioactive compound - evariquinone were estimated against hippocampal HT22 cell death provoked by glutamate. Evariquinone exhibited sturdy defensive effects against glutamate-mediated HT22 apoptosis through the reticence of intracellular reactive

oxygen species accretion and Ca^{2+} influx elicited by glutamate. Evariquinone robustly attenuated glutamate-intervened apoptotic cell death (Song et al., 2018).

Bilobalide is a trilactone isolated from *Pestalotiopsis uvicola* of *Ginkgo biloba* exhibiting neuroprotective effects. The quantity of bilobalide formed by this endophyte was found to be 106 μg/L via HPLC (Qian et al., 2016).

Two compounds (2R,3S)-pinobanksin-3-cinnamate and 15alpha-hydroxy-(22E,24R)-ergosta-3,5,8(14),22-tetraen-7-one, were obtained from *Penicillium sp*. First one exhibited persuasive toxic effects while second one showed compelling defensive effects on corticosterone-treated PC12 cells (Liu et al., 2014).

Chrysogenamide, an alkaloid, was isolated from *Penicillium chrysogenum*, an endophytic fungus. Chrysogenamide demonstrated neuroprotective effects against oxidative stress-stimulated cell death in SH-SY5Y cell lines (Lin et al., 2008).

Geldanamycin is a neuroprotective agent against some of the frequently used drugs like cisplatin, paclitaxel and vincristine that induce neurotoxicity in the neuronal cells of embryos of chick. In this report, in a huge magnitude, geldanamycin collectively with known 17-O-demethylgeldanamycin, and a novel 17-O-demethylgeldanamycin hydroquinone were isolated from a mangrove plant endophyte *Streptomyces sp*. Derivatives of geldanamycin were organized by alteration of C-17 and/or C-19 on the quinone ring and were assessed for *in vitro* activity against P19-derived neurons. Geldanamycin and 19-O-methylgeldanamycin improved endurance and growth of P19-consequential neurons and prohibited neurotoxicity of paclitaxel and vinblastine. 19-O-methylgeldanamycin, having the lowest neurotoxicity and cytotoxicity, is helping as the capable agent in neurodegenerative remedy against neurotoxic anticancer drugs (Tadtong et al., 2007).

Novel bioactive compounds azaphilones and sesquiterpene obatined from endophytic fungus *Nigrospora oryzae* co-cultured with *Irpex lacteus* revealed significant anti-fungal activity with minimum inhibitory concentrations of 16 μg/ml and 128 μg/ml respectively against *Irpex lacteus*. Nigrosirpexin showed AChE inhibitory activity at the very low concentration [50 μM] (Zhou et al., 2018).

One novel monoterpenoid 1-acetoxyisoaustinone and few known dehydroaustin, meroterpenoids, austin, acetoxydehydroaustin, dehydroaustinol and austinol were obtained from endophytic fungus, *Aspergillus* sp. of mangrove plant. It has been found that austin, dehydroaustinol and preaustinoid exhibited AChE inhibitory activity with IC_{50} values of 2.50, 0.40, and 3.00 μM respectively (Long et al., 2017).

Xu et al., 2017 isolated eight compounds from endophytic fungus *Chaetomium sp*. Their chemical structures were assessed through spectroscopy. Azaphilones, armochaetoglobins and xanthenone illustrated modest AChE inhibitory activity with IC_{50} values of 7.34, 5.19, and 4.23 μg/ml respectively.

Eleven strains of endophytes were obtained from stem and roots of *Nerium indicum*. Na et al., 2016 revealed that the strain CH1 showed R_f value which was similar to the standard drug vincamine, a monoterpenoid, advertised as nootropic agent in the management of cerebral anomalies. CH1 has shown significant AChE percentage inhibition with an IC_{50} of 5.16 μg/ml. In conclusion, endophytic microbiota of *Nerium indicum* can be used as substitute source for the synthesis of vincamine and vincamine analogues. One new pyrone derivative along with two novel naphthalenone compounds were obtained from endophytic fungus *Fusarium sp*. Pysarone A exhibited AChE inhibitory activity (Xiao et al., 2018).

Table 1 Endophytic fungi from *Tinospora cordifolia* with therapeutic properties

S.No.	Endophytic fungi	Therapeutic properties	References
1.	*Cladosporium velox*	Antioxidant and genoprotective	Singh et al., 2016
2.	*Cladosporium velox*	Alpha glucosidase inhibitory activity	Singh et al., 2016
3.	*Cladosporium sp.*	Insecticides	Singh et al., 2015
4.	*Nigrospora sp.*	Pesticides	Thakur et al., 2012
5.	*Fusarium sp.*	Anti-gout	Kapoor et al., 2018
6.	*Penicillium sp.*	Antibacterial and anti-tumor activities	Desai et al., 2012
7.	*Fusarium solani*	Anti-carcinogenic	Uzma et al., 2016
8.	*Fusarium culmorum*	Anti-cancer	Sonaimuthu et al., 2010

Table 2 List of natural AChE inhibitors

S.No.	Compounds	Source	References
1.	Harmol	*Peganum nigellastrum*	Zheng et al., 2009
2.	Purpurin	*Rubia cordifolia*	Zengin et al., 2016
3.	Alizharin	*Rubia cordifolia*	Zengin et al., 2016
4.	β-sitosterol	*Polygonum hydropiper*	Ayaz et al., 2017
5.	Berberine	*Coptis chinensis*	Mak et al., 2014
6.	Palmatine	*Coptis chinensis*	Mak et al., 2014
7.	Quercetin	*Quercus alba*	Adedara et al., 2017
8.	Protopine	*Corydalis ternate*	Kim et al., 1999
9.	Malvidin	*Anagallis monelli*	Beara et al., 2017
10.	Chelidonine	*Chelidonium sp.*	Cahlikova et al., 2010
11.	Galantamine	*Galanthus caucasicus*	Santos et al., 2018
12.	Huperzine-A	*H. elmeri*	Santos et al., 2018
13.	Serpentine	*Catharanthus roseus*	Pereira et al., 2010
14.	Decursinol	*Archispirostreptus gigas*	Anand et al., 2012

2.7. Hippocampus

It is an allocortical configuration which is imperative for the coupling of instructions, together with temporary, long-standing and dimensional memory. Communities with widespread bilateral hippocampal injuries are expected to have anterograde amnesia (Squire et al., 1992).

2.8. Scopolamine-induced cognitive anomalies in hippocampus

In this study, fermentation of *Spirulina maxima* was done with *Lactobacillus planetarium* which attenuated scopolamine-induced cognitive abnormalities in mice. *Spirulina maxima* extract showed perfection in cognition, as verified through passive avoidance test (PAT). *Spirulina maxima* extract (400 mg/kg) showed a latency time and an escape latency time of 76.0 and 88.5 sec, respectively in PAT (Choi et al., 2018). It was inferred that *Spirulina maxima* showed memory-improving properties in the hippocampus of scopolamine-administered mice via a rise in ERK signaling and a

chronological stimulation of the appearance of brain derived neurotrophic factor (BDNF) and p-CREB, and these activities are allied to the antioxidant effects of *β*-carotene and other components.

In this study, authors have explored the free radical scavenging and neuroprotective activities of compound K (CK), a ginsenoside in scopolamine-induced memory deficits mice. CK significantly reduced the levels of malondialdehyde while raised the level of catalase in hippocampus. CK showed decrease in neuronal apotosis and Aβ expression in addition to instigation of Nrf2/Keap1 signaling pathway in scopolamine subjected mice. Thus, it can be inferred that CK may have a significance in the treatment of Alzheimer's disease (AD) (Yang et al., 2019).

Diosmin exhibited neuroprotective effects in scopolamine (SCO)-induced cognitive anomalies in animal model. Diosmin (50 and 100 mg/kg) showed increase in bar latency time, latency period and the total time spent in quarter in different behavioral tests. Diosmin revealed significant decrease in TNF-α level and pro-inflammatory mice in hippocampus when compared to SCO administered mice. Thus, Diosmin may be regarded as a potential candidate in the management of dementia (Shabani et al., 2018).

Laminaria japonica, a sea snarl, exhibited learning and memory amelioration that might assist in treatment of common neurodegenerative diseases like dementia. *Laminaria japonica* showed significant reduction in AChE enzymatic activity while increase in level of acetylcholine, ERK1/2 protein in hippocampal brain tissue. Thus, it is concluded that *Laminaria japonica* may serve as a prospective contender in the treatment of memory impairments (Reid et al., 2018).

Sufferers of AD have dementia. SKF83959 showed the significant improvement in various behavioral parameters like Y-maze and Morris water maze test in amnesic mice. SKF restored the scopolamine-induced down-regulation of BDNF in hippocampus but not in cortical region. These studies indicate that SKF could be a new and prospective therapeutic candidate for healing dementia in case of AD (Sheng et al., 2018).

Berte et al., 2018 showed that Taraxerol, a triterpene obtained from leaves of *Eugenia umbelliflora* inhibits AChE both *in vitro* and *in vivo*. Taraxerol showed significant improvement in streptozotocin and scopolamine-induced memory deficits in amnesic mice through different behavioral tests.

Willughbeia cochinchinensis exhibited acetylcholinesterase and butylcholinesterase enzymatic inhibitory activities in scopolamine-induced dementia in experimental mice. W*illughbeia cochinchinensis* inhibited scopolamine-induced cognitive anomalies in the Morris water maze and novel object recognition. *Willughbeia cochinchinensis* showed increase in scopolamine-provoked reduction in novel arm entry in the Y-maze paradigm (Can et al., 2018).

Diisopropylfluorophosphate exhibited anti-AChE activity in addition to significant increase in long term potentiation. Hippocampal cholinergic motion augments long term potentiation of synaptic transmission and controls learning and memory (Masuoka et al., 2019).

Matrine attenuated amnesia induced through scopolamine via anti-acetylcholinesterase and anti-butylcholinesterase activities. Matrine showed decrease in oxidative stress as it reduced the levels of malondialdehyde whereas increase the concentration of anti-oxidant enzymes like superoxide dismutase and catalase. Matrine significantly improved the memory impairments in various behavioral parameters (Sun et al., 2019).

Terminalia chebula Retz. (Combretaceae) is a conventional herbal remedy that is broadly used in the healing of immunodeficiency illness, diabetes mellitus and gastric ulcer in Asia. In this study, *Tinospora cordifolia* showed significant decrease in AChE level while increase in acetylcholine (Ach) and choline acetyltransferase (ChAT) levels in scopolamine-induced amnesia in hippocampus. *Tinospora cordifolia* exhibited anti-oxidative effects via attenuating increased levels of reactive oxygen species, nitric oxide and malondialdehyde (Kim et al., 2018).

Liquiritigenin isolated from *Glycyrrhiza* exhibited neuroprotection and anti-inflammation. In this report, liquiritigenin showed anti-AChE activity. Liquiritigenin enhanced cAMP response element binding besides phosphorylation of extracellular serine-regulated kinase (ERK) and BDNF in the brain tissue of scopolamine subjected mice (Ko et al., 2017).

Soursop fruit extract ameliorates scopolamine-induced cognitive deficits and oxidative harm in the hippocampus of experimental animals. Soursop fruit extract raised the concentration of antioxidants while diminished the amount of the cytochrome c and caspase-3 in hippocampus (Al Omairi et al., 2019).

Jiao-tai-wan, a Chinese drug recommendation cinnamon, is chiefly used for the management of sleeplessness. Oral administration of Jiao-tai-wan attenuated the scopolamine-induced increase and decrease in AChE and ChAT activities. Jiao-tai-wan mitigated oxidative stress via reducing concentration of reactive oxygen species and malondialdehyde while enhancing the amount of superoxide dismutase and catalase in hippocampus (Wang et al., 2018).

Gaps in Study

A. Bioactive secondary metabolites from endophytic fungi have great potential in therapeutics. Very few endophytic fungi have been explored so far in the management of diseases.

B. Till date there is no report on neuroprotective activities of endophytic fungi isolated from *Tinospora cordifolia*.

C. AChE inhibitors from endophytic fungi of *Tinospora cordifolia* have not been studied so far.

D. Pharmacological action of bioactive compounds from endophytic fungi of *Tinospora cordifolia* have not been reported as yet.

Chapter 3 Materials and methods

3.1. Endophytic fungi isolation from *Tinospora cordifolia*

3.1.1. Collection of plant samples, sterilization and isolation of endophytic fungi

Mature healthy leaf samples of *Tinospora cordifolia* were collected from the campus of Thapar Institute of Engineering and Technology, Patiala and stored in sterile bottles. Samples were surface sterilized according to Petrini et al., 1992. Samples were dipped in 70% ethanol for 1min followed by immersion in aqueous solution of 5% NaOCl for 15 minutes. Samples were rinsed in double-distilled sterile water thrice and extra moisture was removed using blotting paper. Leaves were incised into 15-20 segments, measuring approximately 0.5×0.5 cm. Samples were placed on Petri dishes having potato dextrose agar (PDA) supplemented with streptomycin (200 mg/l) followed by incubation at 26 ± 1°C (BOD Incubator) for 10-14 days for the growth of endophytic fungi.

3.2. Purification and coding of isolated endophytes

After the growth of endophytic fungi, culture was purified by placing the hyphal tips on fresh PDA plates. The obtained pure cultures of fungal endophytes were coded as GL15 to GL28 in sequence as they were obtained from Giloy leaf (GL).

3.3. Fermentation and extraction of isolated fungal metabolites

The mycelium plugs from 7-10 day old cultures were slashed and inoculated aseptically into a 500 ml Erlenmeyer flask containing 250 ml of potato-dextrose broth (PDB) and then incubated at 26 ± 1°C for 21 days. The mycelium was separated with the help of muslin cloth from the culture medium and the filtrate was extracted using identical volume of ethyl acetate after 21 days. Collected organic phase was evaporated using rotary evaporator under reduced pressure (IKA, Rota evaporator) (Pedra et al., 2018). The dried crude residues were collected into glass vials and stored at 4^{o}C for further bioassays.

3.4. Preliminary *in vitro* screening for acetylcholinesterase (AChE) inhibition

AChE inhibitory activity was evaluated according to Ellman et al.,1961 with slight modifications. Donepezil (DPZ) was used as reference AChE inhibitor. Five different concentrations of 200, 400, 600, 800 and 1000 µg/ml of each fungal extract (GL15, GL16, GL17, GL18, GL19 and GL20) were used to evaluate percentage inhibition of AChE. 50 µL of

AChE (1.00 U mL^{-1}) and 20 µL of above concentration of fungal extract were incubated in 96 wells plate for 30 min at room temperature. 100 µL (1.5 mM) of DTNB was added in the above solution. Acetylthiocholine iodide (ATCI) (15 mM, 10 µL) was added into it to commence the reaction and absorbance was recorded immediately at 415 nm using ELISA plate reader. The same steps were followed for reference compound DPZ.

$$\text{Percentage inhibition of AChE} = \frac{\text{Absorbance of blank} - \text{Absorbance of sample} \times 100}{\text{Absorbance of blank}} \quad \ldots\ldots(i)$$

3.5. Free radical scavenging assay

Anti-oxidant activity was performed with slight modulations (Chatterjee et al., 2019). 2,2-diphenyl-1-picryl-hydrazyl (DPPH) was dissolved in methanol. Four different concentrations of 100, 250, 500 and 1000 µg/ml of fungal extracts were used to assess the antioxidant activity. Standard compound was ascorbic acid and its concentration was 100 µg/ml. Different concentration of fungal extracts were mixed with 150 µl of 2,2-diphenyl-1picryl-hydrazyl (DPPH) (100µM) and methanol into 96 wells micro titer plate. After 30 minutes of incubation, the absorbance was taken at 517 nm using ELISA plate reader. The readings were recorded in triplicate.

$$\text{Percentage of radical scavenging} = \frac{\text{Absorbance of blank} - \text{Absorbance of sample} \times 100}{\text{Absorbance of blank}} \quad \ldots.(ii)$$

3.6. *In vivo* AChE assay

3.6.1. Selection of animal model

Adult male Swiss Albino mice weighing 18-22 g were collected from IMS, B.H.U. and were housed at 26 ± 2 °C, relative humidity 44–56% and light:dark cycle (12:12) (No.: Dean/2015/CAEC/986). Scopolamine was used to induce dementia in experimental animal model. The experiment was conducted in agreement with the principles of laboratory animal care guidelines.

3.7. Experimental design

AChE inhibitory activity of six fungal extracts i.e. GL15, GL16, GL17, GL18, GL19 and GL20 was measured on the selected animal model. The experimental protocol consists of single set of 8 days experiment. The animals were divided into six groups with six animals each namely control, scopolamine (SCO), GL15 1.25, GL15 2.5, GL15 5.0 and DPZ 3.0. Vehicle was administered intra-peritoneally to control and SCO mice. GL (1.25, 2.5 and 5.0 mg/kg; i.p.) were

administered with GL15 1.25, GL15 2.5 and GL15 5.0 respectively from day 1 to day 7 of experimental schedule. Similarly, DPZ (3 mg/kg; i.p.) was also administered to DPZ-3.0 group from day-1 to day-7. On day-7, 1 hr after fungal extract or reference drug treatment, except for those in control group all the animals were administered with scopolamine (3 mg/kg; i.p.) (Fig. 3). Thereafter, passive avoidance test and Y-maze paradigm were performed. All the behavioral parameters were estimated with ANY-maze^{TM} (version-3.72, USA) video recording software. On 8th day animals were then sacrificed by cervical dislocation and immediately hippocampus was micro-dissected and instantly stored at -80°C for further analysis.

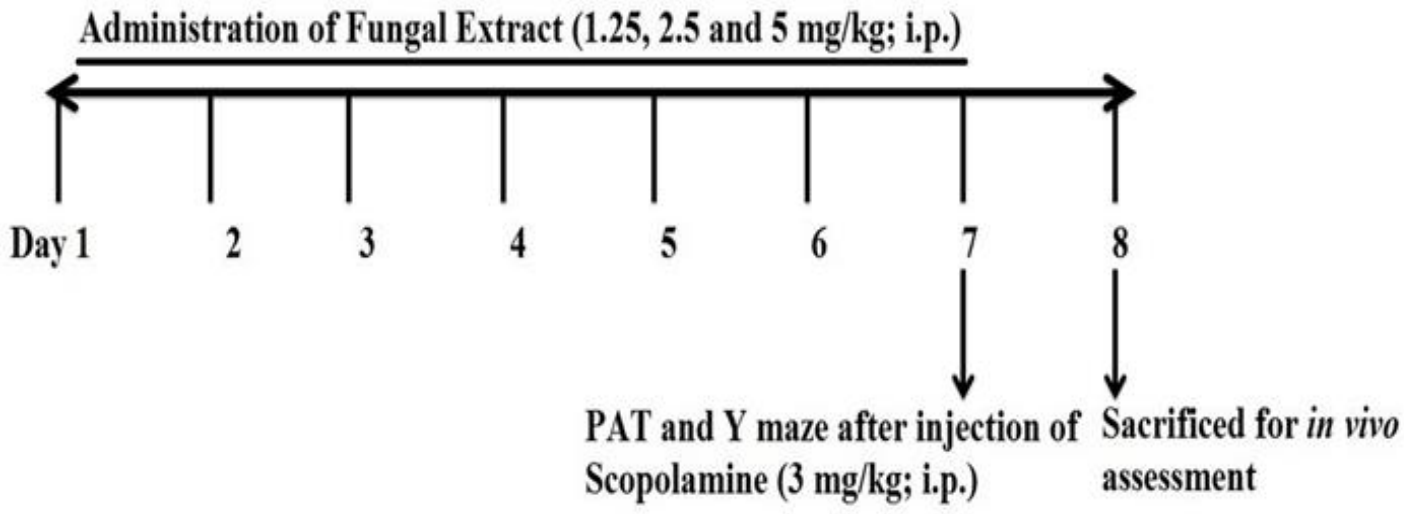

Fig. 3 Experimental design of *in vivo* study of GL15

3.8. Assessment of behavioral performance

3.8.1. Passive avoidance test

The passive avoidance test (PAT) was conducted in an apparatus with two identical compartments (20 × 24 × 30 cm). One compartment was dark, and the other compartment was bright, and outfitted with 2 mm (diameter) stainless steel rods conveying an electrical shock to the animal (Fig. 4). Both compartments were divided by a barrier. PAT was performed during two consecutive days. The acquisition trial took place on day one. After 24 hrs, the retention trial was conceded out to explore the extensive tenure avoidance memory. The latency period was estimated with a maximum time of 300 s and used as an indicator of avoidance memory (Zhang et al., 2018).

Fig. 4 Passive avoidance test compartments

3.8.2. Estimation of memory in Y-maze test

Anxiety-like behavior, spatial recognition memory and general exploratory attitude were estimated as the entire entries in all arms, percentage entries in known and novel arms and the percentage of ratio of time spent in novel arm to time spent in all the arms and in the center of the apparatus respectively were assessed in Y-maze (Fig. 5) (Dellu et al., 1992; Krishnamurthy et al., 2013).

Fig. 5 Y-maze paradigm

3.9. Estimation of AChE receptor through western blot technique

According to Bradford (1976) protein amount was estimated. Bovine serum albumin was used as a standard to make the calibration curve. Hippocampal tissue was electrophoresed in 10% SDS-PAGE gel for AChE, followed by relocation to polyvinylidene fluoride membranes and finally attached with precise antibodies. The membrane was incubated overnight with Rabbit anti-AChE (1:100) polyclonal primary antibodies. Suitable secondary antibodies were taken and probed with

membrane. Results were quantified through ImageJ software.

3.10. Neurochemical analysis

Animals were dissected and hippocampus was isolated after conclusion of the behavioral study on 8th day. The hippocampus was dissolved in 10 mM phosphate buffer and centrifuged. For the further estimation of AChE concentration in hippocampal tissue supernatants were taken. AChE was measured in the hippocampus of scopolamine subjected animals by Ellman's method. 100 µL of the supernatant was incubated with 100µL of ATCI (15 mM) in presence of phosphate buffer for 5 min. The results were evaluated at 415 nm after addition of 100 µL of 1.5 mM DTNB.

3.11. Histopathological studies

The hippocampus was isolated from scopolamine administered mice. Mixing of brain tissues occurred in 10% formalin followed by sectioning in paraffin blocks. Eosin and haematoxylin dyes were used to stain section and ultimately photographs were captured via phase contrast microscope at 40x magnification.

3.12. Preliminary qualitative analysis of crude extract GL15

Phytochemical screening of crude fungal extract GL15 was done to explore the occurrence of diverse classes of natural compounds in the extract (Hadacek et al., 2000).

3.12.1 Protocol for Screening

3.12.2. Test for alkaloids

Wagner's test: 2-3 drops of Wagner's reagent were added to 1 ml of the fungal extract. A reddish-brown precipitate will show the presence of alkaloids.

3.12.3. Test for tannins and phenols

1ml of ethylacetate extract was added to tube possessing 2 ml of 5 % of alcoholic ferric chloride solution. Blue-black precipitate will confirm the test positive for tannins and phenols.

3.12.4. Test for steroids and terpenoids

Salkowoski's reaction: 1 ml of ethylacetate fungal extract was added to test tube having 10 ml chloroform and 1 ml acetic anhydride. After that, 2-3 drops of concentrated sulphuric acid was added to above mixture. Green ring will show the existence of steroids while formation of yellow color shows the presence of terpenoids.

3.12.5. Test for amino acids

Ninhydrin test: 1 ml of fungal extract was added to 5-6 drops of ninhydrin reagent and heated over boiling water bath for 5 min. Purple coloration will indicate a test positive for amino acids.

3.12.6. Tests for carbohydrates

Molisch's test: 2 drops of alcoholic solution of α- naphthol were mixed with 1 ml of fungal extract. After shaking the mixture vigorously for few seconds, 3-4 drops of concentrated sulphuric acid were added slowly along the sides of the test tube. The occurrence of violet ring at the junction will show the presence of carbohydrates.

3.12.7. Tests for fixed oils and fats

Saponification test: a drop of phenolphthalein and 2-3 drops of 0.5N potassium hydroxide were mixed with 1 ml of fungal extract and heated on a water bath for 1-2 hours. Soap formation will confirm the existence of fixed oils and fats.

3.13. Purification of crude extracts

3.13.1. Thin layer chromatography (TLC)

TLC is a straightforward and rapid method to discover the quantity of constituents present in a crude extract. The ethylacetate extract of endophytic fungus GL15 was spotted higher than 2 cm from the bottom of TLC plates (Silica Gel F_{254}-Merck). Optimized mobile phase was used for running of samples on TLC plates. The mobile phase alienated the elements into various ranges of R_f values. The developed chromatogram was visualized under UV light at 365 nm (Harir et al., 2019).

3.13.2. Optimization of mobile phase

Universal approach for optimizing the mobile phase in TLC is to amend the solvent strength according to polarity index so that R_f value could be in the range of 0.15-0.85 (Table 3). Solvents were used in pure form. Finally, gradients of chloroform, methanol and ethylacetate were used for running of extract on TLC plates.

Table 3 Polarity index for various solvents

Relative polarity	Compound formula	Group	Representative solvent compounds
Nonpolar	R-H	Alkanes	Petroleum ethers and hexanes
	Ar-H	Aromatics	Toluene and Benzene
	R-O-R	Ethers	Diethyl ether
	R-X	Alkyl halides	Tetrachloromethane and chloroform
	R-COOR	Esters	Ethyl acetate
	R-CO-R	Aldehydes and Ketones	Acetone and methyl ethyl ketone
	$R-NH_2$	Amines	Pyridine and triethylamine
	R-OH	Alcohols	Methanol, ethanol and isopropanol
	$R-CONH_2$	Amides	Diethylformamide
	R-COOH	Carboxylic acids	Ethanoic acid
Polar	H-OH	Water	Water

Increasing Polarity

3.14. Purification of different fractions of GL15 through column chromatography

3.14.1. Preparation of sample

Ethylacetate extract of the fermented culture of endophytic fungus was evaporated to dryness, weighed and pulverized. 50 mg of sample was used for separation of various fractions.

3.14.2. Preparation of column

The column preparation incorporated adsorption of the extract, charging and dissemination of column. The extract chosen for fractionation was adsorbed on stationary phase. Glass column with suitable measurement was chosen based on the magnitude of sample to be separated. Chosen column was rinsed with solvent to eliminate impurities. A cotton pad was positioned decisively at the base to avert the current of stationary phase. The column was charged with stationary phase by wet packing method. Subsequent layer of cotton pad was positioned above the mixture to avoid messing of stationary phase while adding eluting solvents from pinnacle of column. The slurry was discharged smoothly on the apex of column to shun the assembly of air bubbles and packed with mild forced air. The column was then rinsed with hexane and then geared up by administration of sufficient quantity of the first solvent mixture through it. Crude extract was suspended in hexane then loaded onto column. The column was then eluted with a 100% hexane, gradients of chloroform and ethylacetate: 100% chloroform, chloroform:ethylacetate (9:1), chloroform:ethylacetate (8:2), chloroform:ethyl-acetate (7:3), chloroform:ethylacetate (6:4), chloroform:ethylacetate (5:5). Finally, cleaning was done with pure methanol (Andriana et

al., 2019). Test tubes were used to collect eluted solvents from the column. Each fraction was concentrated and spotted on a TLC plate. The TLC plate was developed with mobile phase – chloroform and ethylacetate and visualized under UV 365 nm. On the basis of TLC profile analogous fractions were pooled together. These pooled fractions were evaporated to obtain dried fractions.

3.15. Screening of bioactive fractions

The fractions were subjected to AChE inhibitory activity as discussed in section 3.14.2. The fraction showing maximum percentage inhibition was selected for further characterization to identify the bioactive compounds present in it.

3.16.1 Characterization of fraction exhibiting maximum AChE percentage inhibition

3.16.2. UV-visible spectroscopic evaluation of bioactive fraction 3 of GL15

Ultravoilet absorption spectroscopy is the quantization of lessening of a ray of a light once it surpasses all the way through a sample. Absorption dimensions can be at a particular wavelength or above a comprehensive spectral range. UV-Vis spectrometer-2600, Japan was turned on and lamps were allowed to warm up for an appropriate period of time to soothe them. Cuvette was filled with 100% methanol which served as a blank. Reading for the blank was set as zero. Cuvette was filled with the sample. Both sample and standard compound quercetin were dissolved in 100 % methanol. For the certainity of results, the cuvette was rinsed twice with the sample and three-fourth portion of cuvette was filled with it. Cuvette was positioned in the spectrophotometer in the accurate trend. The region between 190 to 380 nm is called as the UV region while from 380-900 nm is recognized as visible region of the spectrum. Readings were taken from 190-800 nm (Catauro et al., 2015).

3.17 Analysis of fraction 3 of GL15 through fourier-transform infrared spectroscopy

3.17.1. KBr Pellet method followed for solid samples

2 mg of sample was taken in fine powder form on spatula along with 0.25-0.50 teaspoons of potassium bromide pellets. Components were mixed together using pestle and mortar. Grinding was done properly. The appropriate amount of sample was placed to cover base in pellet die. After that mixture was placed in press at 5000-10000 psi. After pressing, sample was positioned in fourier transform infrared spectroscopy (FTIR) sample holder. The range of infrared spectrum was from 400 to 4000 cm^{-1}. Analysis was done through Perkin Elmer RX FTIR, USA at SAIF-

labs, Punjab University, Chandigarh. The peaks of sample were recorded. FTIR spectrum of bioactive fraction was recorded as percentage of light transmitted vs wavenumber (Catauro et al., 2015).

3.18. Electrospray ionization mass spectrometry (ESI-MS) and ESI (MS/MS) of bioactive fraction 3

Analysis of mass spectrometry was carried out on Waters Alliance 2795 with electrospray ionization in positive mode. Bioactive fraction 3 was dissolved in solvent mixture Acetonitrile: Water:Methanol::7:1:2. 20 µl of sample was injected into C18 column having flow rate of 1ml/min. The supply pressure of nitrogen and argon were 6-7 bar and 5-6 bar respectively. Capillary voltage was 2650V while collision energy was 4ev. The cone voltage was 30V. The collision energy for MS-MS was 15-20ev. Desolvation gas was set to be 550ltrs/hr while desolvation temperature was 300^{o}C. The source temperature was 110^{o}C. Finally, mass spectra were documented (Gill et al., 2019).

3.19. Identification of endophytic fungus GL15 by microscopic and molecular methods

3.19.1. Identification of endophytic fungus through morphology

Lactophenol cotton blue staining was performed to explore the structure of hyphae, spore morphology, texture and colony morphology of endophytic fungi. Microslide was placed in laminar hood and a single drop of dye was put on it followed by addition of endophytic fungal hyphal from PDA plate. The piercing of fungal tissue was done followed by placing of cover slip on it and carefully observed for the hyphal structure and spores under phase contrast microscope (Ranganathan et al., 2019).

3.19.2. Molecular based identification of endophytic fungus

The mycelium plugs were cut from endophytic fungus and put into 500 ml flask containing PDB. The flask was incubated at 26 ± 1^{o}C in shaker with rpm of 80 for 7 days. On 7th day the mycelia was filtered using muslin cloth and dried in an oven to remove moisture and then crushed using liquid nitrogen and stored at -80^{o}C for genomic DNA isolation**.**

3.19.3. DNA extraction using CTAB method

100 mg of crushed fungal tissue was taken in a 2ml centrifuge tube. 600 µl of preheated extraction buffer was added to the tube followed by incubation at 65^{o}C for 60 min. Centrifugation at 13,500 g for 20 min at 4^{o}C was done to remove debris. The resultant supernatant was

transferred to fresh microfuge tube. 800 µl of Phenol:Chloroform:Isoamyl Alcohol (25:24:1) was added to the supernatant containing tube. Centrifugation at 13,500 g for 20 min at 4^{o}C was done to obtain aqueous layer. After collecting aqueous layer in fresh tube, 800 µl of isopropanol was added to it in order to precipitate DNA. Pellet was collected after centrifugation at 13,500 g for 20 min at 4^{o}C. Ethanol (70%) was added to above centrifuge tube followed by centrifugation at 13,500 g for 20 min at 4^{o}C. Supernatant was discarded and pellet was dissolved in 25 µl of sterile MQ water (Latiffah et al., 2018). The DNA so obtained was checked by running in 0.8 % agarose gel. Agarose powder (0.32) was weighed and mixed with 40 ml of 0.5X TBE buffer after heating. Ethidium bromide (2 µl) was added to it. Mixture was poured into casting tray with comb placed in it. Gel was allowed to solidify at room temperature. Comb was removed and tray was placed in electrophoresis chamber.

3.19.4. Polymerase chain reaction (PCR)

ITS regions were amplified using forward primer ITS1 and reverse primer ITS4. A reaction mixture of volume 25 µl to perform PCR. PCR consists of three steps with a preliminary denaturation at 95°C at 2 min and 35 cycles of 30 s at 95°C, annealing at 55°C for 30 s and extension at 72° for 1 min. Purification of amplified PCR product was done using QIA quick PCR purification kit, purchased from Qiagen India limited. 1 kb ladder and PCR samples were loaded in gel electrophoresis unit for evaluation. Quantification of PCR product was done with the help of nanodrop. Nanodrop was calibrated using millipore water. After that 1 µl of sample was loaded and concentration of PCR product and A_{260}/A_{280} value were recorded.

3.19.5. Sequencing of sample

PCR product was then sequenced by employing sanger sequencing. BioEdit Sequence Alignment Editor Version 7.0.5 software was used for sequencing (Mishra et al., 2012).

3.19.6. Sequence analysis of ITS region

Sequences obtained were then searched for sequence similarity with the non-redundant database maintained by NCBI. Homology in the sequence was searched by comparing sequence of interest with already available data using BLAST tool. Similar sequences were aligned using ClustalW. Neighbor joining method was used to construct the phylogenetic tree in Mega X software (Tamura et al., 2007).

3.20. Statistical analysis

All results were shown as mean ± standard errors of mean (S.E.M.). Two-way ANOVA followed by Bonferroni post hoc test was executed to assess arm bias behavior between known and novel arm in Y-maze paradigm. All additional statistical analysis of data was carried out by using One-way ANOVA followed by Tukey's multiple comparison post hoc test. $P<0.05$ was considered as significant.

Chapter 4 Results

In the present study, medicinal plant *Tinospora cordifolia* was selected for the isolation of endophytic fungi. The endophytic fungal extracts were screened for acetylcholinesterase inhibitory activity. The above plant was chosen for study as not much work has been reported on the isolation of endophytic fungi from *T. cordifolia*.

4.1. Sample collection

Leaf samples of *Tinospora cordifolia* were collected from the campus of Thapar Institute of Engineering and Technology, Patiala and stored in sterile bottles (Fig. 6).

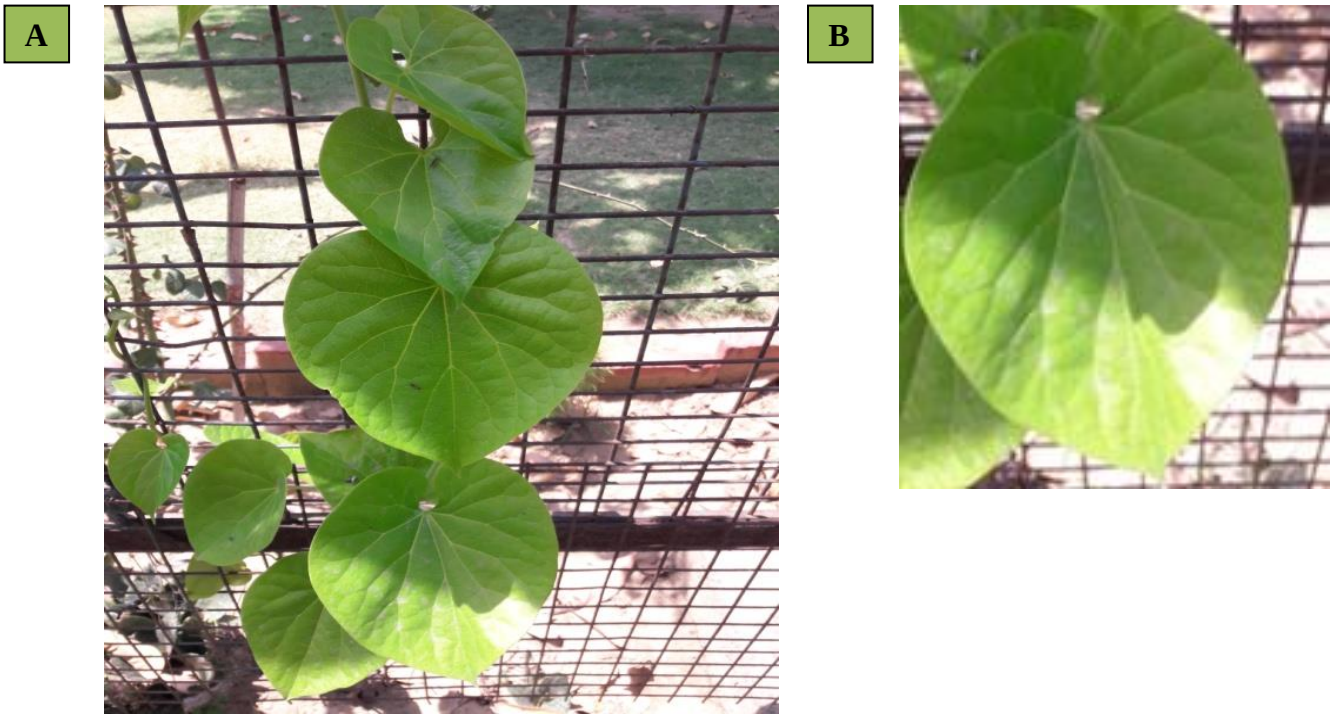

Fig. 6 (A) Shrub of *T. cordifolia* (B) Leaf of *T. cordifolia*

4.1.1. Isolation of endophytic fungi from medicinal plant *Tinospora cordifolia*

Leaf samples were placed on Petri dishes having potato dextrose agar (PDA) supplemented with streptomycin (200 mg/l) followed by incubation at 26 ± 1°C (BOD Incubator) for 10-14 days for the growth of endophytic fungi. The plates were observed regularly for the growth of endophytic fungi. A total of 14 different types of endophytic fungi were obtained from the leaves of *Tinospora cordifolia* and these were named as GL15-GL28 (Fig. 7).

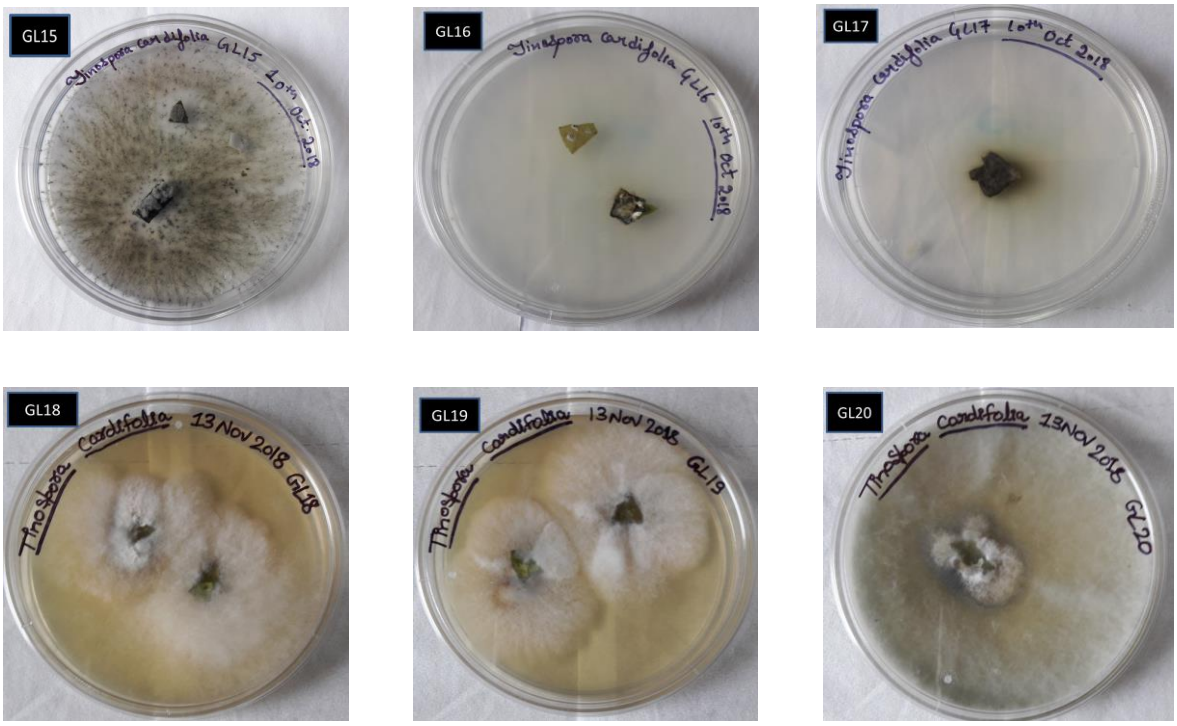

Fig. 7 Fungal isolates from *Tinospora cordifolia* (GL15-GL20).

4.2. Purification of fungal isolates

Purification of the culture from the mixed population was done to get the pure strains (Fig. 8). Culture was purified by placing the hyphal tips on PDA plates. Plates were then incubated at 26 ± 1°C. After the growth of endophytic fungi, the master cultures were stored at 4°C for further use.

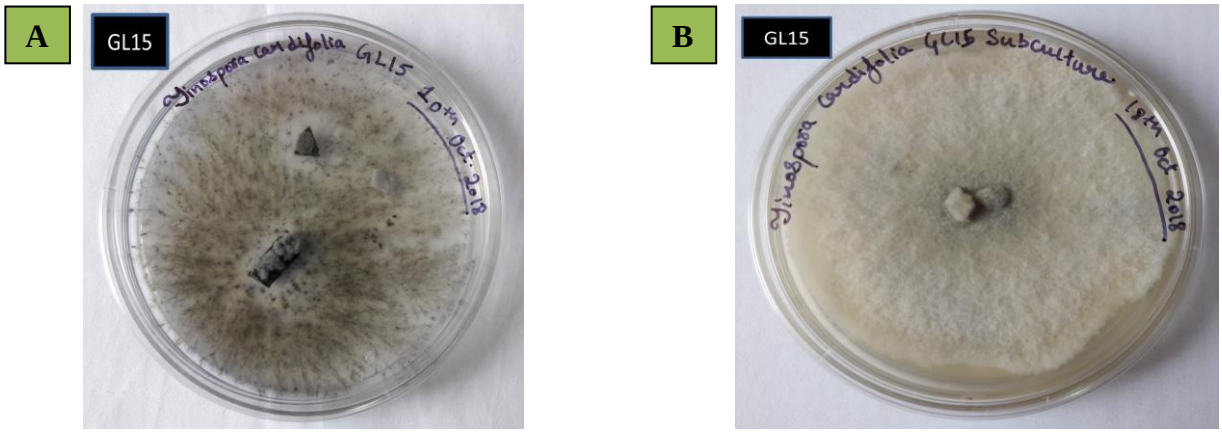

Fig. 8 (A) Endophytic fungi from leaf of *T. cordifolia* (B) Pure isolate obtained from *T. cordifolia*.

4.3. Fermentation and extraction of fungal metabolites from endophytic fungi

The purified fungal isolates GL15-GL20 were inoculated in PDB and kept at 26 ± 1°C for 21 days in stationary condition. After 21 days of fermentation, the mycelia was separated using muslin cloth from the culture medium. The dried weight of mycelia after drying in hot air oven to constant weight was recorded (Table 4). The broth obtained after filtration was extracted with equivalent volume of ethylacetate. Crude extracts were obtained via rotary evaporation of collected ethylacetate phase. The crude endophytic fungal extracts were stored in glass vials at 4^{o}C for conducting bioassays (Fig. 9).

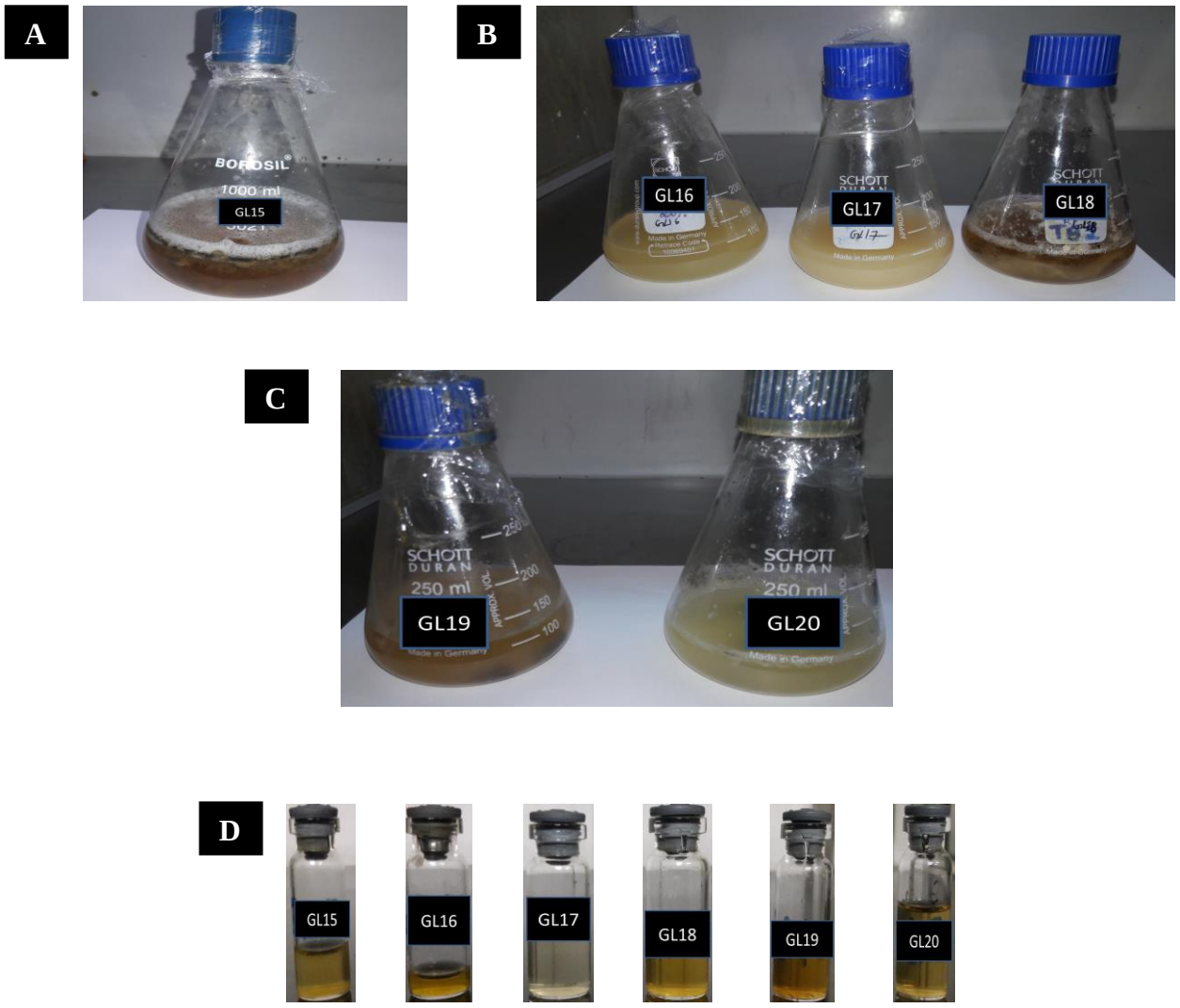

Fig. 9 (A), (B) and (C) Fermentation broth after 21 days (D) Crude extracts obtained from endophytic fungi.

Table 4 The dried weight of mycelia of isolated endophytic fungi

Extracts	Dry mycelial weight (mg)
GL15	340
GL16	160
GL17	400
GL18	150
GL19	200
GL20	420

4.4. Preliminary *in vitro* screening for acetylcholinesterase (AChE) inhibition

The crude extracts were solubilized in DMSO to obtain different concentrations of each fungal extract (GL15, GL16, GL17, GL18, GL19 and GL20). Donepezil (DPZ) was used as a reference drug at a concentration of 80 µg/ml. This assay involves AChE break down of acetylcholine into choline and acetic acid. Choline binds with DTNB and gives yellow color. In the presence of AChE inhibitor white color forms because choline does not bind with DTNB. Percentage AChE inhibition shown by extracts GL15-GL20 was calculated.

4.4.1. Effect of fungal extracts on acetylcholinesterase (AChE) inhibition

The percentage inhibition of AChE by six fungal extracts (GL15, GL16, GL17, GL18, GL19 and GL20) is shown in Fig. 10. One-way ANONA showed that there were considerable variations among groups in GL15 [$F(5, 12) = 71.62$; $P<0.05$]. GL15 showed percentage inhibition of 60.64, 70.77, 82.79, 88.23 and 91.45 at 200, 400, 600, 800 and 1000 µg/ml respectively. GL16 showed percentage inhibition of 27.75, 28.49, 29.47, 32.88 and 34.56 at 200, 400, 600, 800 and 1000 µg/ml respectively. GL17, GL18, GL19 and GL20 did not show any considerable activity. GL15 exhibited a significant activity of 91.45% at 1000 µg/ml which was quite comparable with that of DPZ (80 µg/ml).

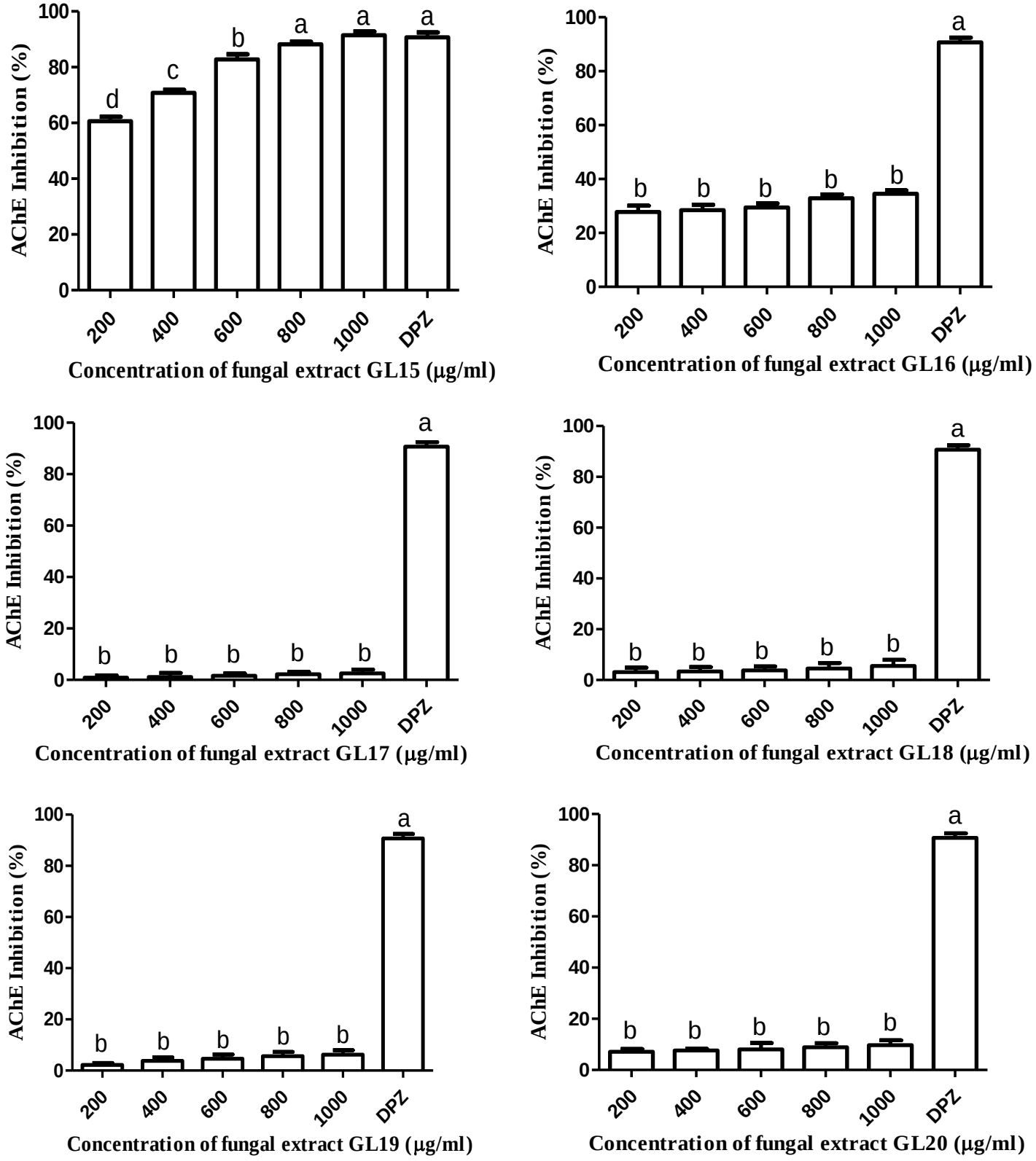

Fig. 10 *In vitro* acetylcholinesterase (AChE) inhibitory potential of GL15, GL16, GL17, GL18, GL19 and GL20. Bars showing a common letter within the treatments are not significant at $P<0.05$

4.5. *In vitro* free radical scavenging assay

Four different concentrations of 100, 250, 500 and 1000 µg/ml of fungal extracts GL15-GL20 were used to evaluate the antioxidant activity. Standard compound was ascorbic acid (AA) and its concentration was 100 µg/ml. Different concentration of fungal extracts were mixed with 150 µl of 2,2-diphenyl-1-picryl-hydrazyl (DPPH) (100µM) and methanol into 96 wells micro titer plate. DPPH is violet in color but if the scavenging of free radical occurs then yellow color appears which implies that extract has shown antioxidant activity.

4.5.1. Assessment of anti-oxidant activity by fungal metabolites

The anti-oxidant effects of GL15, GL16, GL17, GL18, GL19 and GL20 are shown in Fig. 11. One-way ANOVA showed that there were significant variations in antioxidant activity among groups in GL15 [$F(4, 10) = 552.9$; $P<0.05$], GL16 [$F(4, 10) = 77.51$; $P<0.05$], GL19 [$F(4, 10) = 139.4$; $P<0.05$] and GL20 [$F(4, 10) = 427.9$; $P<0.05$]. GL15 showed percentage scavenging activity of 7.19, 40.46, 54.88 and 59.62 at 100, 250, 500 and 1000 µg/ml respectively. GL16 showed percentage scavenging activity of 9.85, 19.72, 40.33 and 62.31 at 100, 250, 500 and 1000 µg/ml respectively. GL19 showed percentage scavenging activity of 32.41, 45.40, 51.54 and 62.34 at 100, 250, 500 and 1000 µg/ml respectively. GL20 showed percentage scavenging activity of 3.20, 4.73, 6.62 and 69.22 at 100, 250, 500 and 1000 µg/ml respectively. GL17 and GL18 did not show any anti-oxidant activity. GL15, GL16, GL19 and GL20 showed maximum anti-oxidant activity at 1000 µg/ml which was analogous to that of AA (100 µg/ml) (Fig. 12).

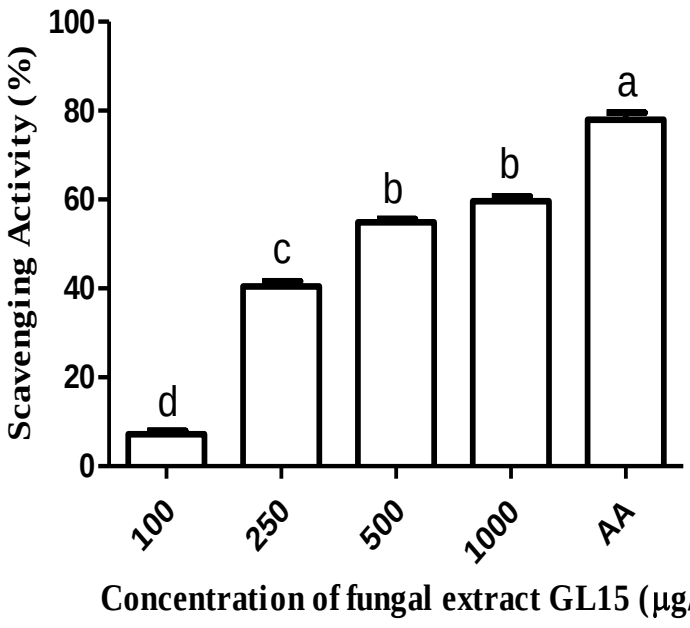

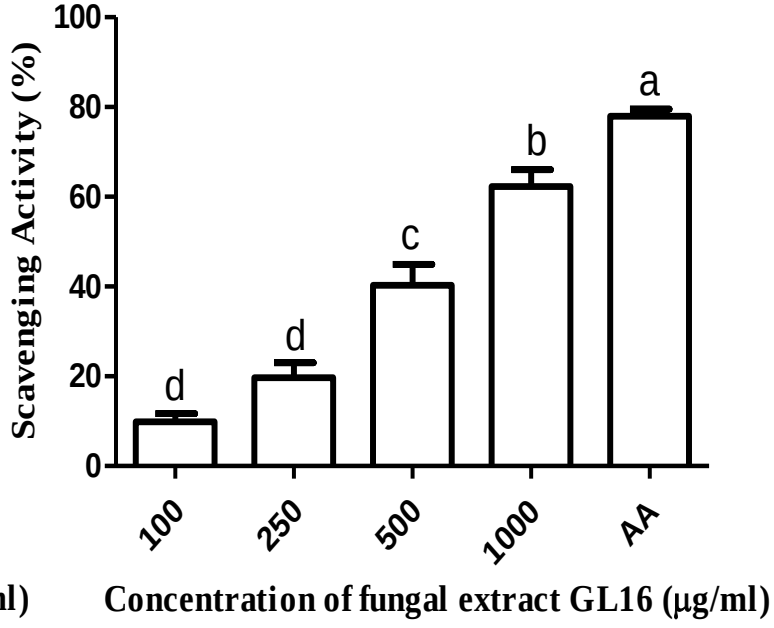

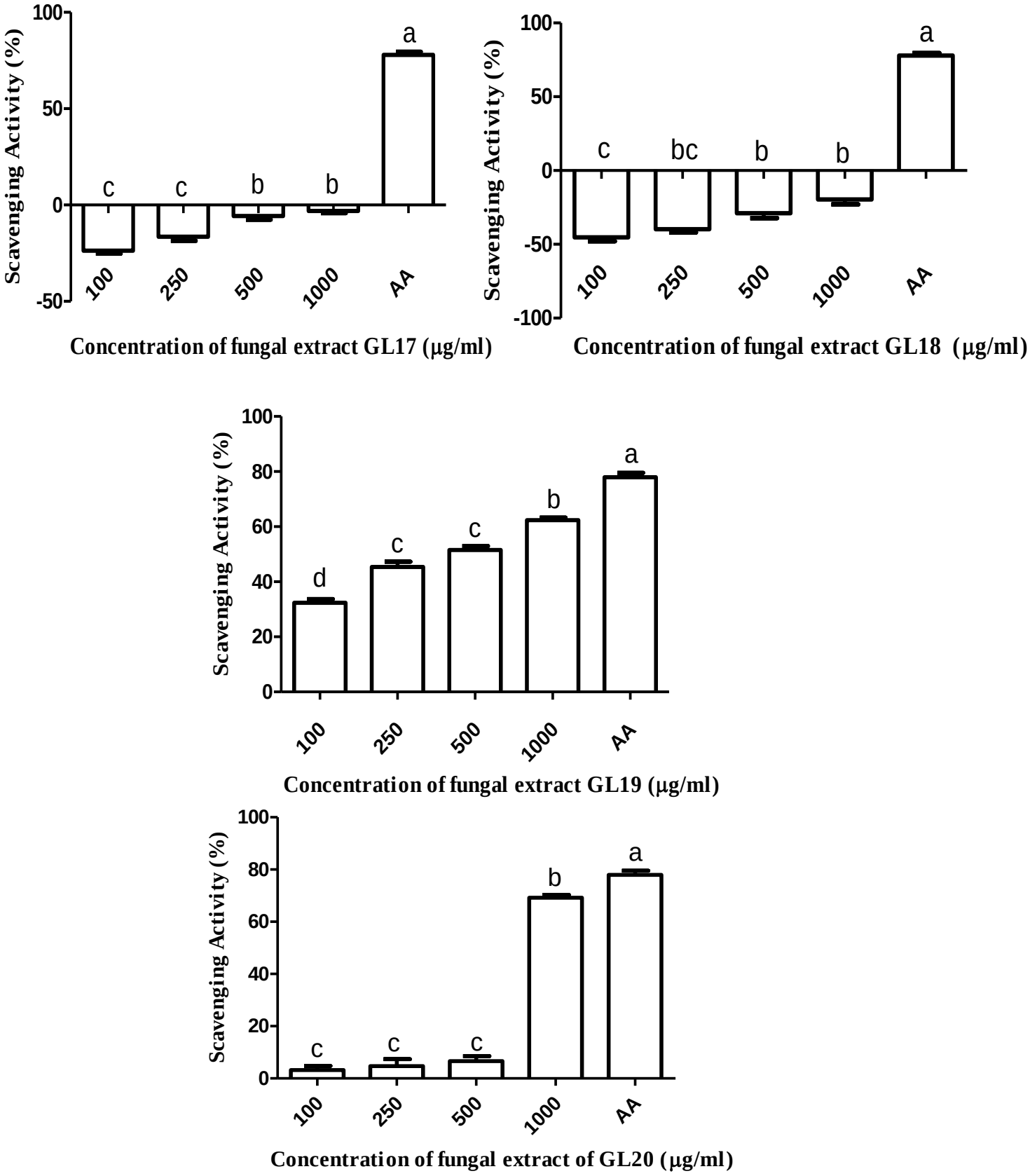

Fig. 11 *In vitro* free radical scavenging activity by GL15, GL16, GL17, GL18, GL19 and GL20. Bars showing a common letter within the treatments are not significant at $P<0.05$.

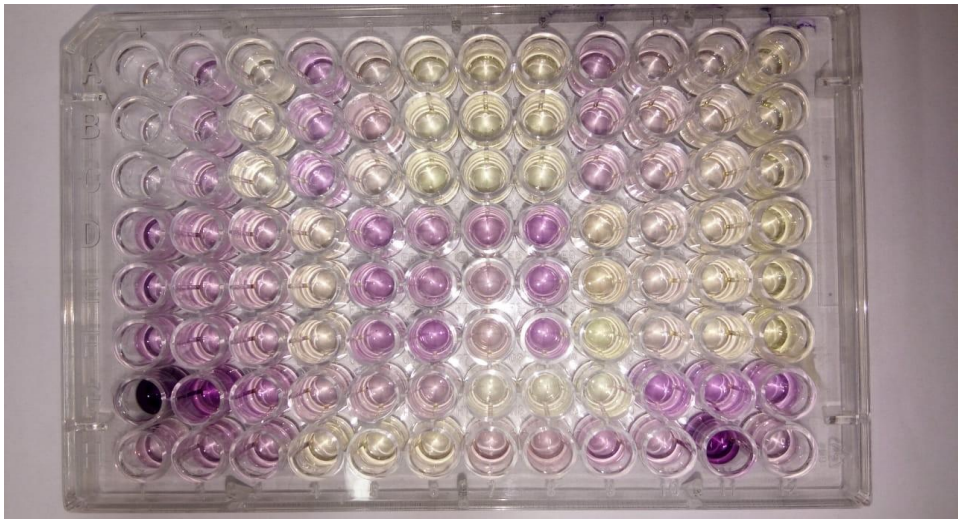

Fig. 12 Radical scavenging activity of extracts (GL15-GL20) in 96 wells ELISA plate.

4.6. Assessment of behavioral performance

Out of six fungal extracts only GL15 exhibited significant anti-AChE activity of 91.45% at concentration of 1000 µg/ml. GL15 also showed anti-oxidant activity of 59.62% at a concentration of 1000 µg/ml. Therefore, GL15 was further chosen for *in vivo* AChE evaluation. Mice were divided into six groups with six animals each namely control, SCO, GL15 1.25, GL15 2.5, GL15 5.0 and DPZ 3.0. Vehicle was administered intra-peritoneally to control and SCO mice. The experimental mice were administered with GL (1.25, 2.5 and 5.0 mg/kg; i.p.) from day 1 to day 7 of experimental schedule. Similarly, DPZ (3mg/kg; i.p.) was also administered to mice from day-1 to day-7. On day-7, 1 hr after fungal extract or reference drug treatment, except for those in control group all the animals were administered with scopolamine (3mg/kg; i.p.). Thereafter, passive avoidance test (PAT) and Y-maze test were performed.

4.6.1. Estimation of cognition in passive avoidance test (PAT)

The PAT was conducted in an apparatus with two alike compartments to estimate the latency period in scopolamine subjected mice.

4.6.2. Effect of fungal extract GL15 on scopolamine (SCO)-induced changes in PAT

The effect of GL15 (1.25, 2.5 and 5.0 mg/kg) and DPZ (3 mg/kg) on SCO-induced alterations in PAT is revealed in Fig. 13. One-way ANOVA showed that there were significant variations in latency period among groups in (B) retention trial [$F (5, 25) = 0.7431$]. SCO decreased the latency period compared to vehicle administered mice. Further, GL15 (5 mg/kg) and DPZ

attenuated the SCO-provoked memory impairments in terms of increase in latency period in mice during PAT. Moreover, there was no dissimilarity between the GL15 5.0 and DPZ mice.

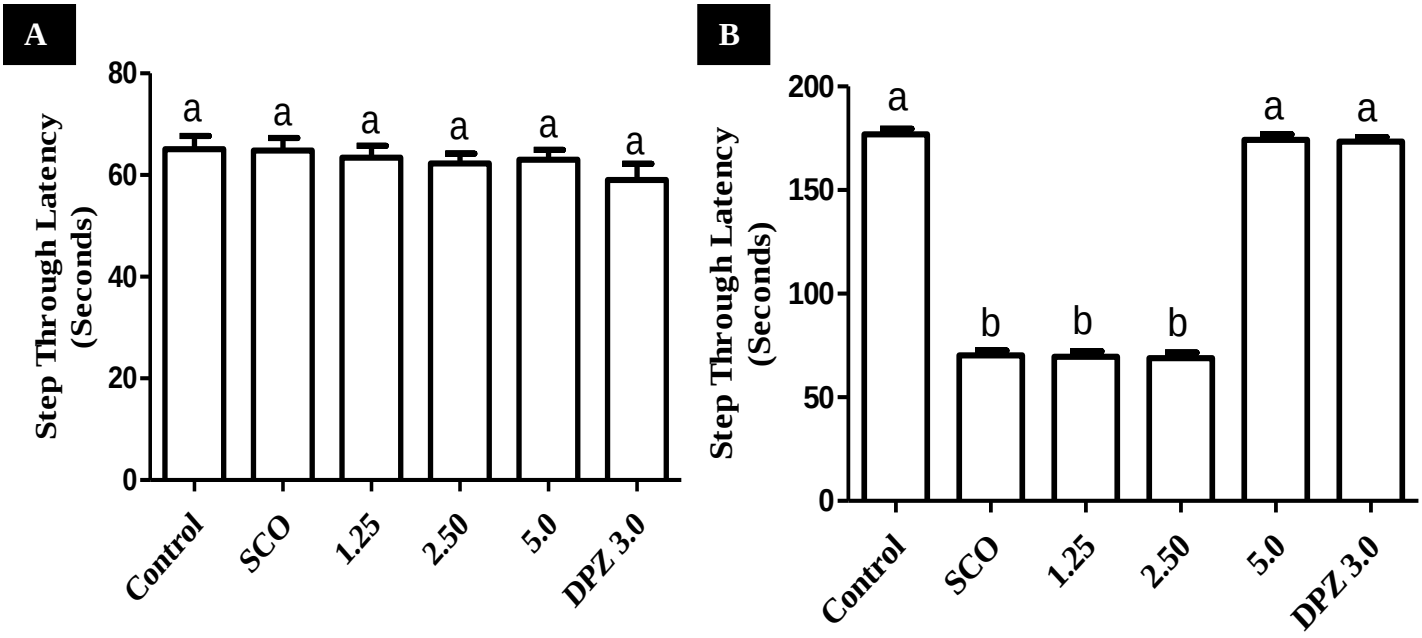

Fig. 13 Effect of GL-15 on alterations in latency period of (A) acquisition trial and (B) retention trial in dementia subjected mice. Bars showing a common letter within the treatments are not significant at P<0.05.

4.6.3. Estimation of memory in Y-maze test

Anxiety-like behavior, spatial recognition memory and general exploratory attitude were assessed in Y-maze paradigm in dementia subjected mice.

4.6.4. Effect of fungal extract GL15 on SCO-provoked loss in memory

The effect of GL15 (1.25, 2.5 and 5.0 mg/kg) and DPZ (3 mg/kg) on SCO-induced alterations in (A) total arm entries in trials 1 (B) total arm entries in trial 2 (C) spatial recognition memory and (D) coping behavior to novel arm in Y-maze test (Fig. 14). There were significant variations in trial-1 and trial-2 among groups [$F(5, 30) = 15.33$; $P < 0.05$] and [$F(5, 30) = 29.81$; $P < 0.05$] respectively). GL15 (5 mg/kg) attenuated the SCO-provoked decrease in total arm entries in trial 1 and trial 2. However, there was no considerable difference between the highest dose of GL15 and DPZ treated animals. Similarly to this, there were no significant variation in coping behavior to novel arm [$F(5, 30) = 1$; $P<0.05$] among groups. Two-way ANOVA revealed considerable dissimilarities for arm bias behavior among groups [$F(5, 60) = 46.49$; $P<0.05$], arm [$F(1, 60) =$

13.25; P<0.05] and major interaction between groups and arm [F (5, 60) = 1.091; P<0.05]. SCO caused increase and decrease in amount of entries into known and novel arm respectively. GL15 (5 mg/kg) and DPZ ameliorated the SCO-provoked cognitive deficits in terms of increase in percentage of entries in novel arm. In contrast, highest dose of GL15 showed much elevated progress compared to DPZ.

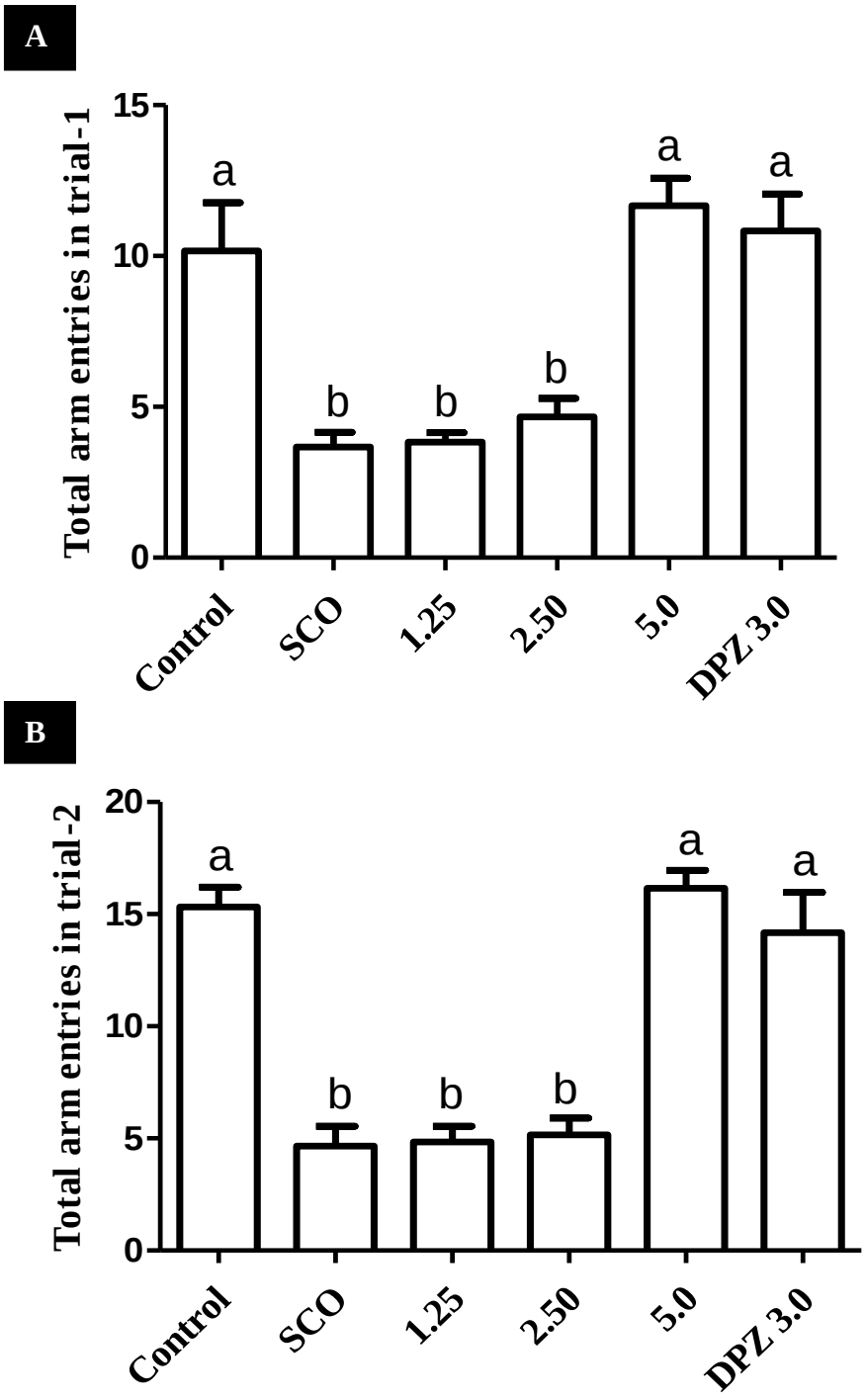

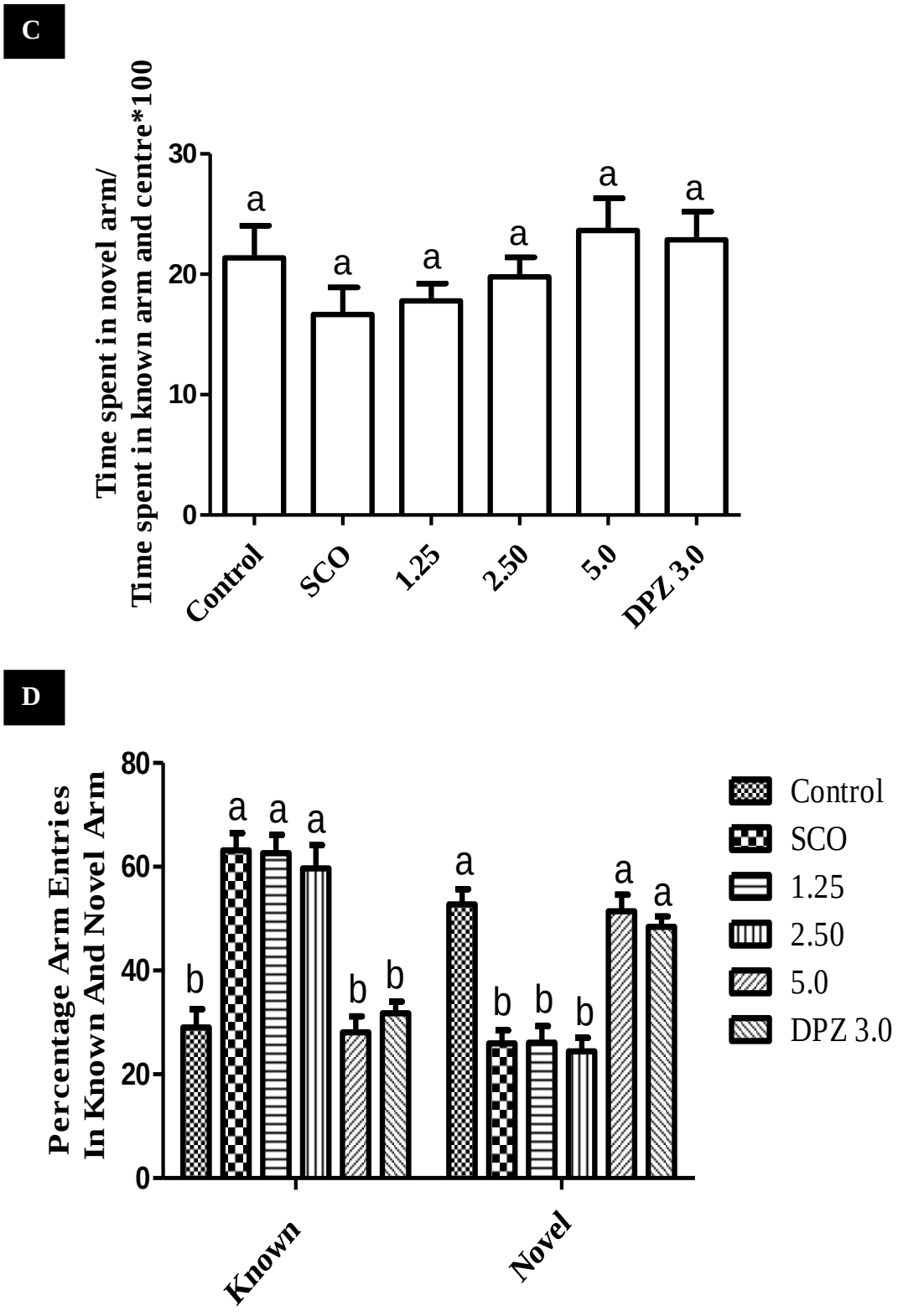

Fig. 14 Effect of GL15 on the total arm entries in trials 1 (A), total arm entries in trial 2 (B), spatial recognition memory (C) and coping behavior to novel arm (D) in SCO subjected mice in Y-maze paradigm. Bars showing a common letter within the treatments are not significant at $P<0.05$.

4.7. Estimation of AChE receptor through western blot technique

On 8th day after behavioral study, animals were sacrificed by cervical dislocation and immediately hippocampus was micro-dissected and expression of AChE receptor was assessed.

4.7.1. Assessment of fungal extract GL15 on hippocampal AChE expression level

The effect of GL15 (1.25, 2.5 and 5 mg/kg) on SCO-provoked alteration in the level of AChE in dementia subjected mice (Fig. 15). One-way ANOVA exhibited that there were significant variations in the level of expression of AChE in hippocampus [F (5, 12) = 28.02; P<0.05] among groups. SCO increased the level of AChE compared to vehicle administered animals. GL15 (5 mg/kg) significantly reversed the SCO-provoked increase in level of AChE. In contrast, DPZ showed no significant variation compared to effective dose of GL15.

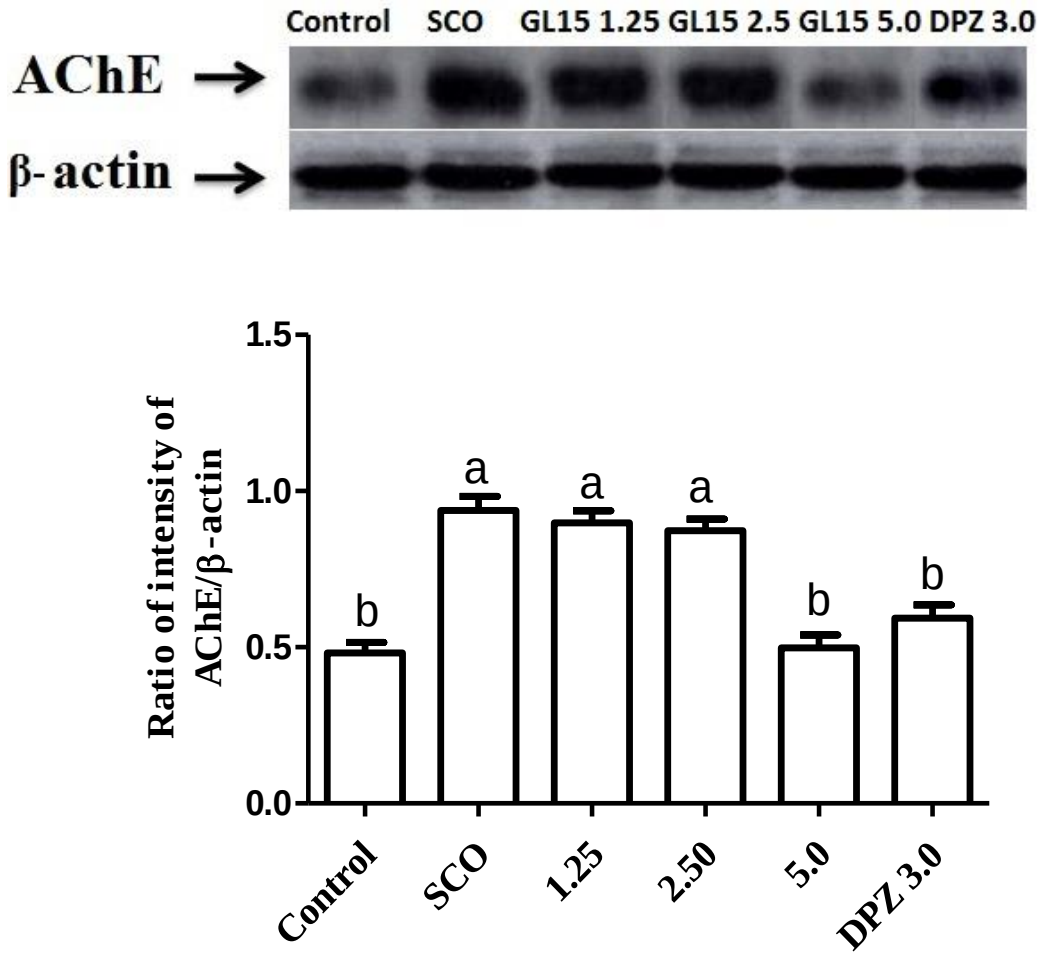

Fig. 15 The effect of GL15 and DPZ on SCO-induced modifications in expression of AChE in hippocampus. Bars showing a common letter within the treatments are not significant at P<0.05.

4.8. Neurochemical analysis

Animals were dissected and hippocampus was isolated after conclusion of the behavioral study on 8th day. The hippocampus was dissolved in 10 mM phosphate buffer and centrifuged. For the further estimation of AChE concentration in hippocampal tissue supernatants were taken.

4.8.1. *In vivo* assessment of AChE in hippocampus of experimental mice

Effect of fungal extract GL15 (1.25, 2.5 and 5 mg/kg) and DPZ (3 mg/kg) on hippocampal AChE concentration in SCO subjected mice is shown in Fig. 16. One-way ANOVA exhibited that there were significant variations in the concentration of AChE in hippocampus [$F(5, 6) = 164.3$; $P<0.05$] among groups. There was significant raise in amount of AChE compared to control mice. Further, highest dose of GL15 showed the improvement against SCO-induced alteration in amount of AChE which was equivalent to that of the reference drug donepezil.

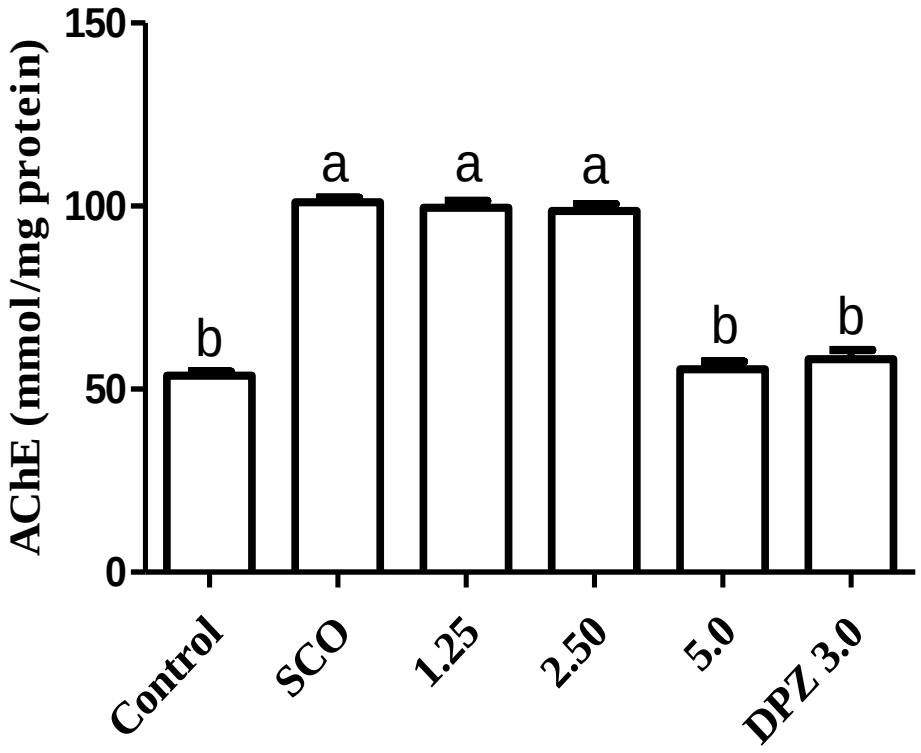

Fig. 16 Effect of fungal extract GL15 and DPZ on SCO-induced changes in amount of AChE in hippocampus. Bars showing a common letter within the treatments are not significant at $P<0.05$.

4.9. Histopathology assessment

Animals were dissected and hippocampus was isolated after conclusion of the behavioral study on 8th day for histopathological evaluation.

4.9.1. Effect of fungal extract GL15 on histopathology in dementia subjected mice

Histopathological alterations in hippocampus of experimental mice are shown in Fig. 17. Hematoxylin and eosin bind with nucleic acid and cytoplasmic membranes respectively. Hematoxylin confers blue color while eosin confers red color. There was a significant difference among groups. Scopolamine administered animals exhibited decrease in level of the neurons in addition to attenuation in cytoarchitecture of hippocampal tissue. Further, GL15 (5 mg/kg) reversed the scopolamine-provoked changes in number of neurons. However, least and median dose of fungal extract did not show any considerable variation in contrast to scopolamine treated mice.

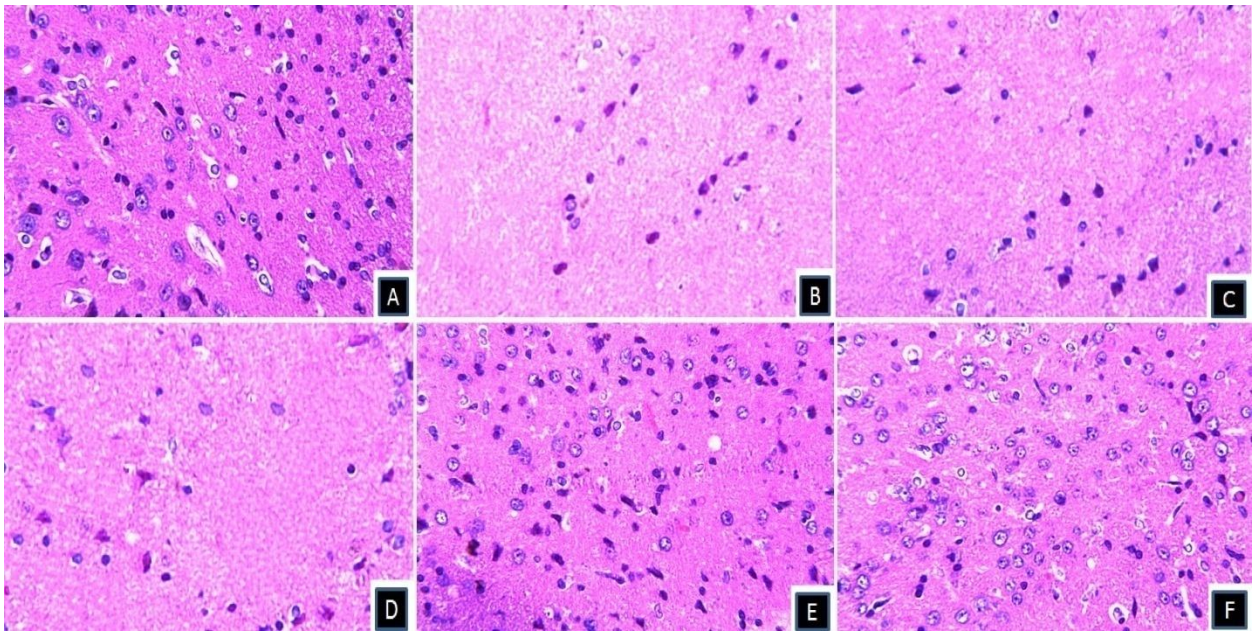

Fig. 17 Histopathological observation of treatment effect of GL15 on SCO-induced cognitive deficits (haematoxylin and eosin staining). (A) Control mice: Section of hippocampus with organized structure and normal number of neuronal cells, (B) scopolamine treated mice; (C) GL15 1.25 and (D) GL15 2.5: Section of hippocampus with disrupted structure and abnormal number of neurons; (E) GL15 5.0 and (F) DPZ 3.0: Section of hippocampal tissue depicted recovery in cytoarchitecture and amount of neurons.

4.10. Preliminary qualitative analysis of crude extract GL15

Fungal extract GL15 exhibited the presence of terpenoids and alkaloids while carbohydrates, phenols, steroids, amino acids, tannins and fixed oils were confirmed as negative (Fig. 18). The presence of terpenoids was confirmed through the formation of yellow color during salkowoski's

test while appearance of reddish brown precipitate during wagner's test confirmed the presence of alkaloids (Table 5).

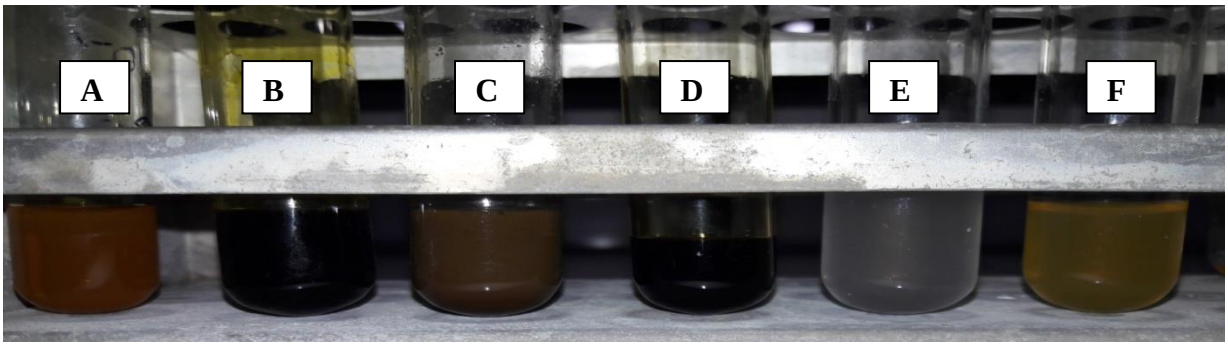

Fig. 18 Phytochemical analysis of miscellaneous classes of photochemical compounds in GL15. (B) Reddish brown precipitate confirmed the presence of alkaloids (F) Formation of yellow color showed the presence of terpenoids

Table 5 Qualitative evaluation of phytochemicals

S.No.	Compounds	Fungal extract GL15
1.	Alkaloids	(+++)
2.	Tannins and phenols	(-)
3.	Terpenoids	(+++)
4.	Steroids	(-)
5.	Amino acids	(-)
6.	Carbohydrates	(-)
7.	Fixed oils and fats	(-)

(+) Positive test, (-) Negative test

4.11. Purification of crude extract GL15

TLC was performed on the crude extract obtained from endophytic fungus GL15. Extract was dissolved in methanol and spotted on Silica Gel F_{254} plates. Different solvent system were optimized according to the polarity of the solvents for separation of fractions from the crude extract (Table 6).

Table 6 Solvent system used for separation of fungal crude extract GL15

S.No.	Sample	Solvent system	Ratio of solvents	No. of fractions	R_f values
1	GL15	Chloroform	100%	2	0.67, 0.65
2	GL15	Ethylacetate	100%	1	0.88
3	GL15	Methanol	100%	1	0.86
4	GL15	Hexane	100%	0	-
5	GL15	Dichloromethane	100%	0	-
6	GL15	Acetic acid	100%	1	0.96
7	GL15	Water	100%	0	-

Further optimization of the solvent system was done by running the crude extract in the combination of solvents listed in the table 7. Solvent system chloroform:ethylacetate (60:40) led to separation of bands R1, R2, R3 and R4 with R_f values of 0.49, 0.59, 0.63 and 0.87 respectively (Fig. 19).

Table 7 Solvent system used for separation of compounds in GL15

S.No.	Sample	Solvent system	Ratio of solvents	No. of fractions	R_f values
1	GL15	Chloroform:methanol	90:10	1	0.65
2	GL15	Chloroform:methanol	80:20	1	0.67
3	GL15	Chloroform:ethylacetate	90:10	1	0.72
4	GL15	Chloroform:ethylacetate	70:30	2	0.67, 0.46
5	GL15	Chloroform:ethylacetate	60:40	4	0.49,0.59, 0.63, 0.87

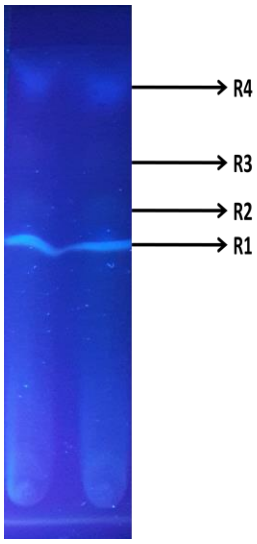

Fig. 19 Fractions of GL15 using chloroform:ethylacetate (60:40) as seen under UV lamp of wavelength 365 nm.

4.12. Purification of crude extract GL15 through column chromatography

30g of silica gel G, 60-120 mesh size was dissolved in 100% hexane and loaded onto the column of length 60 cm and diameter 25 mm. Nine fractions were obtained with following eluents:- F1 in 100% chloroform, F2 in chloroform:ethylacetate (9:1), F3 in chloroform:ethylacetate (8:2), F4-F6 in chloroform:ethylacetate (7:3), F7 in chloroform:ethylacetate (6:4), F8 in chloroform:ethylacetate (5:5) and F9 after washing the column with 100% methanol (Fig. 20). These fractions were pooled together and were evaporated to obtain dried fractions. These nine dried fractions were further subjected to AChE inhibitory activity.

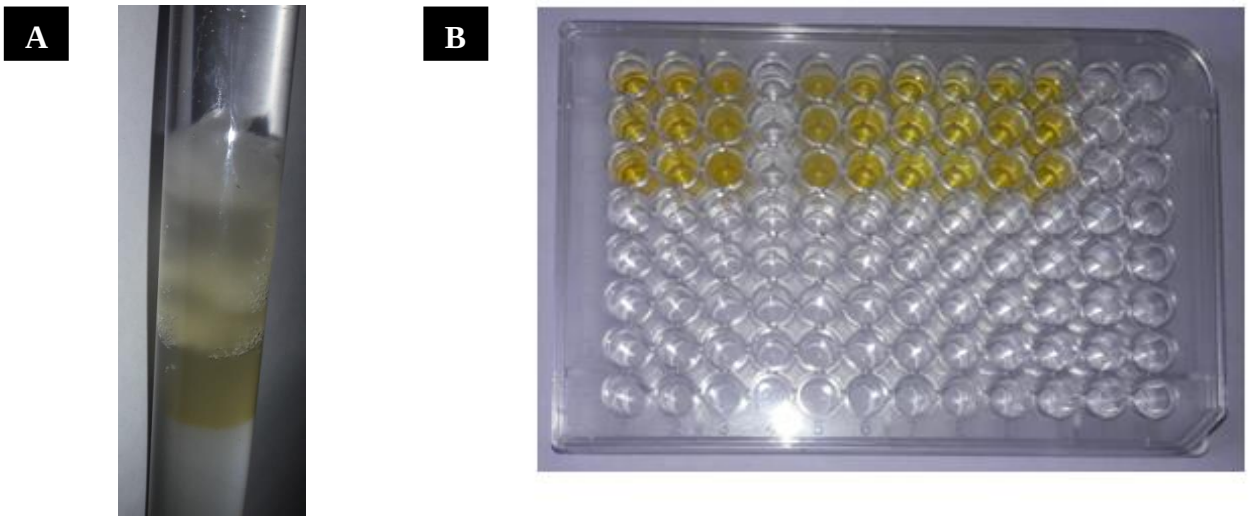

Fig. 20 (A) Separation of crude extract GL15 into different number of fractions (B) AChE inhibitory activity in 96 wells plate.

4.12.1. Assessment of bioactive fractions after purification of crude extract GL15 with column chromatography

The anti-AChE effect of nine fractions obtained from column chromatography of crude extract of GL-15 is shown in Fig. 21. The concentration of each fraction was 1000 µg/ml while that of reference compound DPZ was 80 µg/ml. One-way ANOVA showed that there were significant variations in percentage inhibition of AChE among groups [F (9, 20) = 50.64]. Fraction number three was the most bioactive fraction and exhibited significant percentage inhibition of 87.1%. Fraction 3 exhibited a significant activity of 87.1% at 1000 µg/ml which was quite comparable with that of DPZ (80 µg/ml). Other fraction showed AChE inhibition in the range of 4 to 30%.

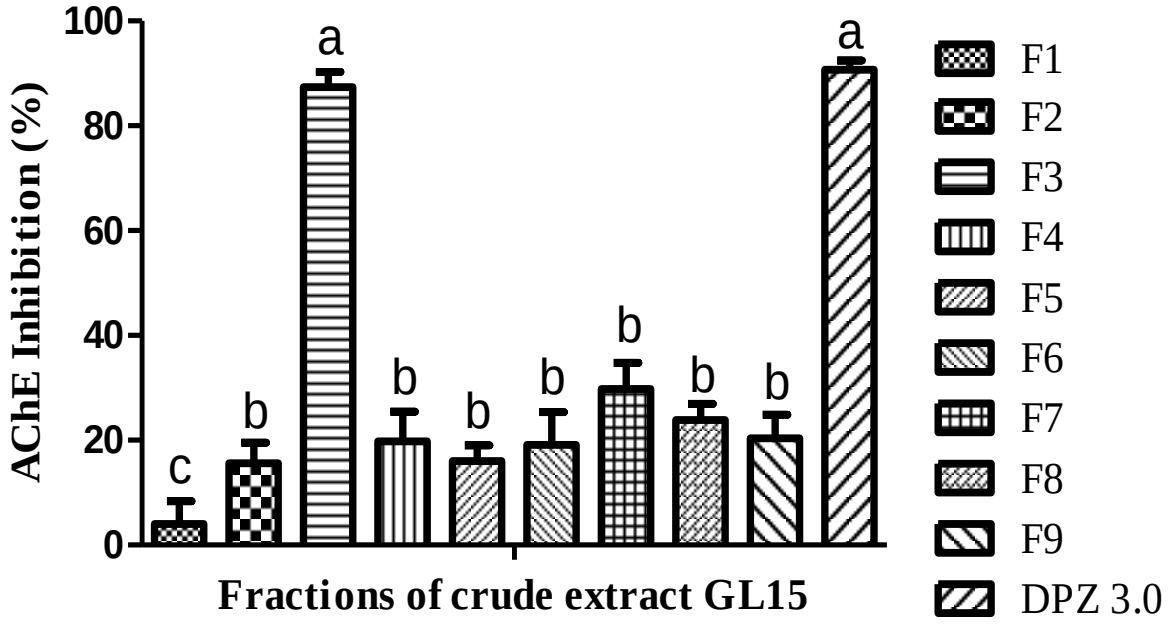

Fig. 21 Effect of nine fractions of GL15 on percentage inhibition of acetylcholinesterase *in vitro*. Bars showing a common letter within the treatments are not significant at P<0.05.

4.13. UV absorption spectrum of bioactive fraction 3

Sample was dissolved in 100 % methanol. Absorbance was taken from 190-800 nm. Fraction 3 showed λ max at 258 nm and 376 nm while reference compound quercetin showed showed λ max at 258 nm and 372 nm (Fig. 22). As the absorbance peaks of fraction 3 and quercetin were similar it may indicate the presence of quercetin in fraction 3 of GL15.

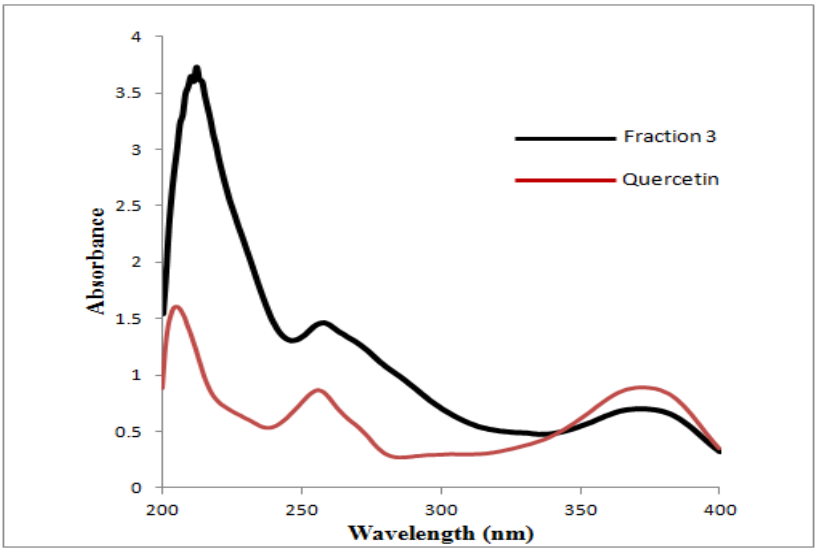

Fig. 22 UV absorbance spectra of fraction 3 and quercetin

4.14. Fourier transform infrared spectroscopy (FTIR) of fraction 3

The range of FTIR spectrum was from 400 to 4000 cm^{-1}. Analysis was done through Perkin Elmer RX FTIR, USA. FTIR spectrum of bioactive fraction 3 of GL15 was recorded (Fig. 23). The FTIR spectrum of bioactive fraction showed a broad peak in the region of 3410.2 which was due to presence of hydroxyl group. The peak at 1664.2 region is due to the presence of carboxyl group. The alkene and ether group were observed at region 1610.8 and 1263 respectively (Table 8). FTIR spectrum of fraction 3 of GL15 showed wave numbers which were quite similar to that of standard quercetin.

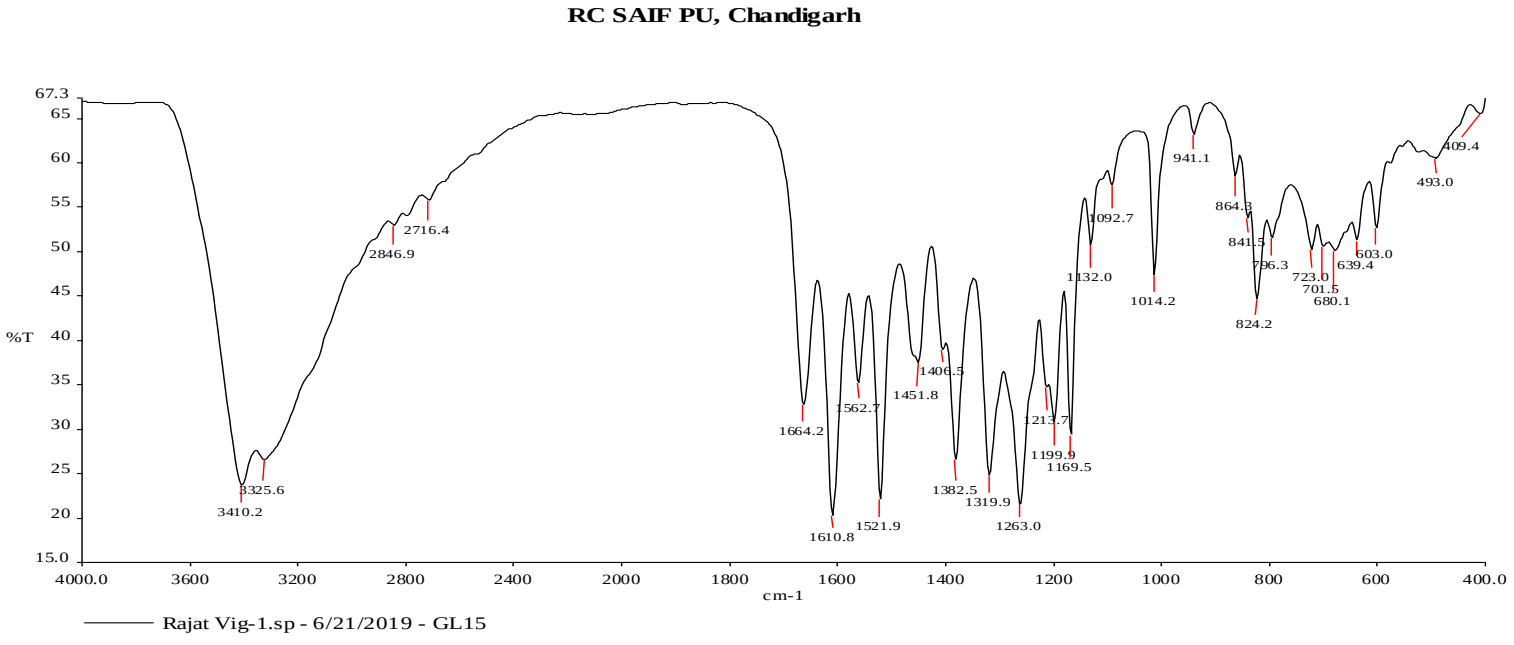

Fig. 23 FTIR spectrum of fraction 3 of GL15

Table 8 FTIR data of fraction 3 of crude extract GL15

S.No.	Wave number	Functional groups
1.	3410.2	OH groups (hydroxyl)
2.	1382.5	OH bending of phenolic group
3.	1664.2	C=O (carboxyl)
4.	1610.8	C=C (alkene)
5.	1562.7	C=C (alkene)
6.	1319.9	C-H in aromatic rings (alkane)
7.	824.2	Out of plane twisting groups
8.	680.1	Out of plane twisting groups
9.	603.0	Out of plane twisting groups
10.	1263.0	C-O in aryl ether ring
11.	1199.9	C-O broadening in phenol
12.	1169.5	C-CO-C twisting in ketone

4.15. ESI-MS/MS analysis of bioactive fraction 3

ESI-MS spectrum of quercetin showed the presence of parent ion at m/z value of 303.10 (Fig. 25). Reported m/z $[M+H]^+$ value of quercetin is 303.04 Theoretical molecular mass of quercetin is 302.236 g/mol. Molecular formula of quercetin is $C_{15}H_{10}O_7$ (Fig. 24). Peaks of fragment ions 153.04, 137.06 and 229.08 were recorded in ESI-MS/MS spectrum of quercetin (Fig. 26). A parent ion of m/z 303.20 was recorded in ESI-MS analysis of bioactive fraction 3 (Fig. 27). ESI-MS/MS spectrum of fraction 3 recorded parent ion peak of 303.22 (Fig. 28). Based upon the analysis and review of literature it may be inferred that fraction 3 of GL15 contains quercetin (Table 9).

Table 9 ESI-MS and ESI-MS/MS analysis of GL15 (fraction 3) and standard quercetin data

	Quercetin	**Fraction 3**
m/z $[M+H]^+$	303.04	303.22
Product ions (MS/MS)	153.04, 137.06 and 229.08	-
Molecular weight	302.23g/mol	302.23 g/mol
Molecular formula	$C_{15}H_{10}O_7$	$C_{15}H_{10}O_7$
Compound	Quercetin	Quercetin
Reported bioactivity	Anti-AChE	Anti-AChE
References	Mass Bank	Mass Bank

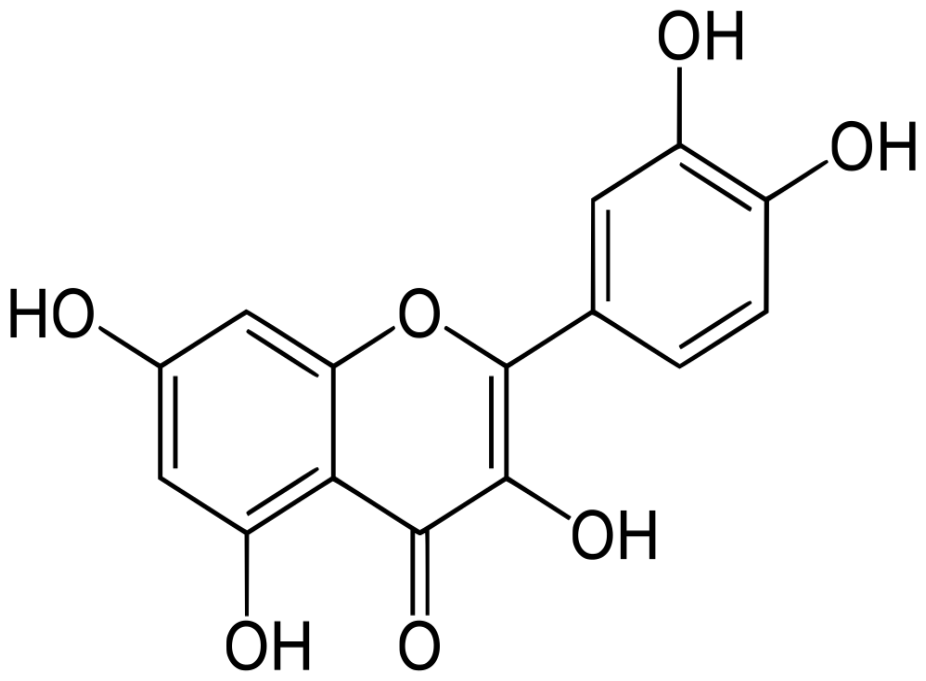

Fig. 24 Structure of quercetin

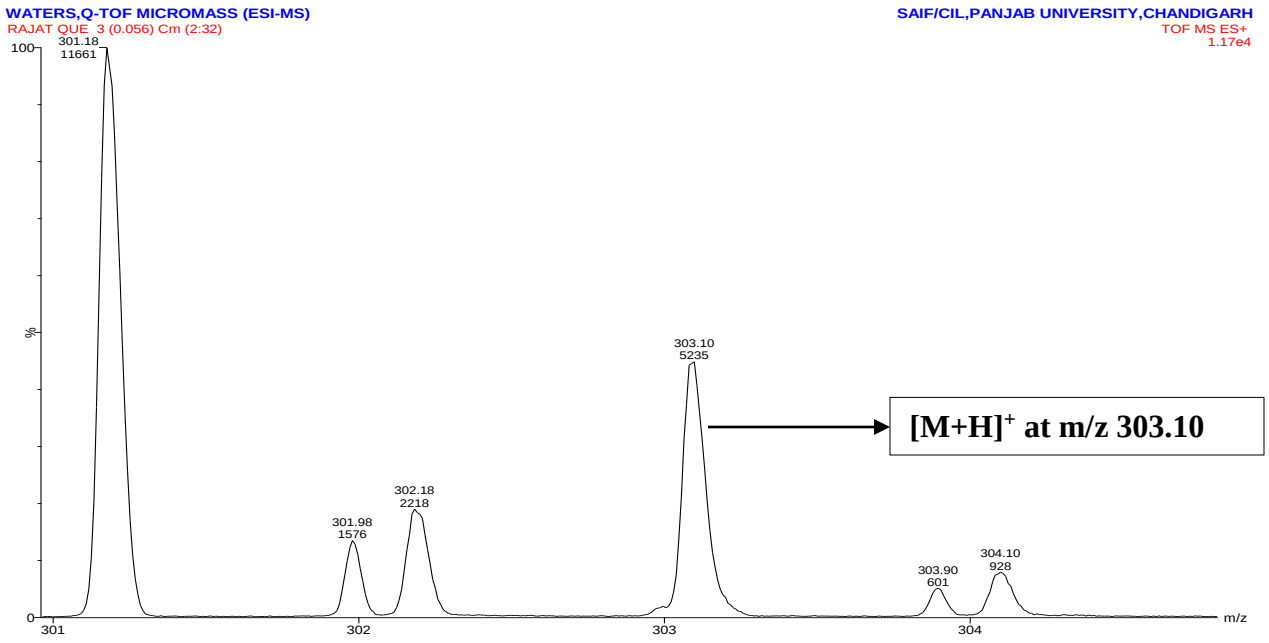

Fig. 25 ESI-MS spectrum of reference compound quercetin

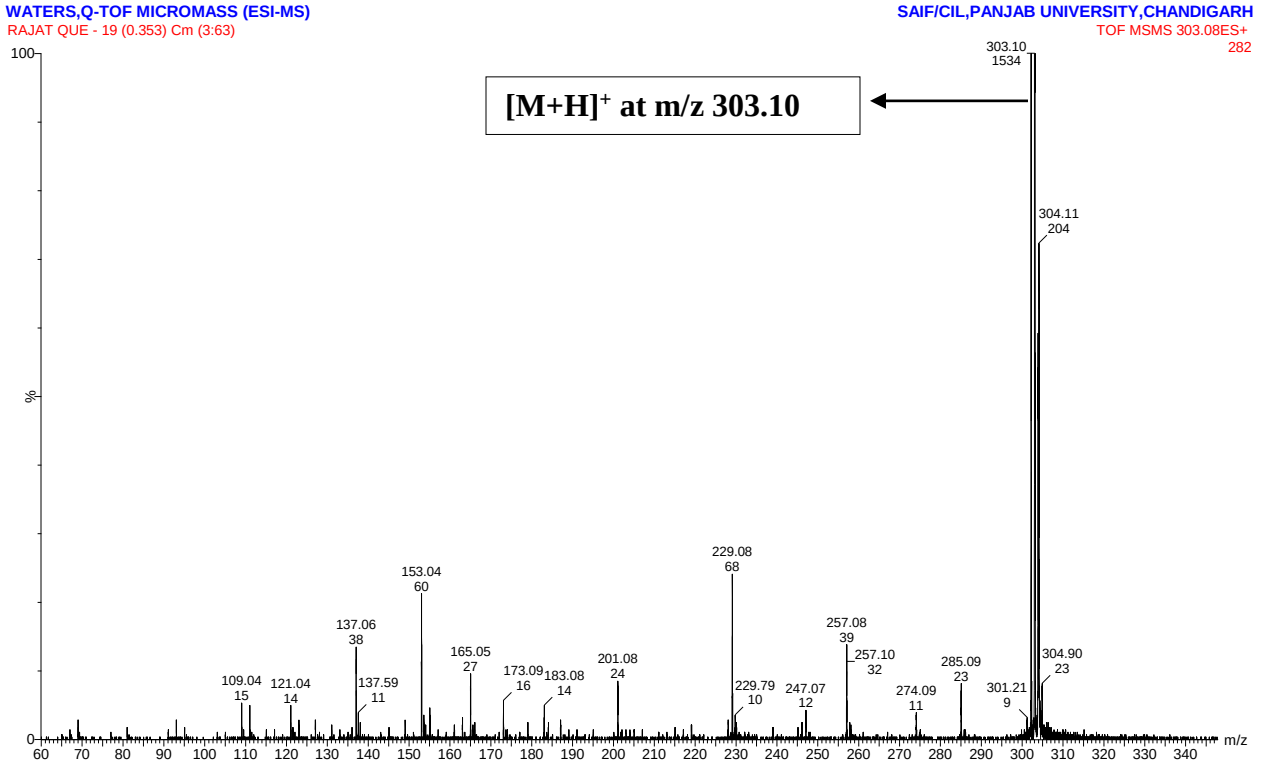

Fig. 26 ESI-MS/MS spectrum of reference compound quercetin

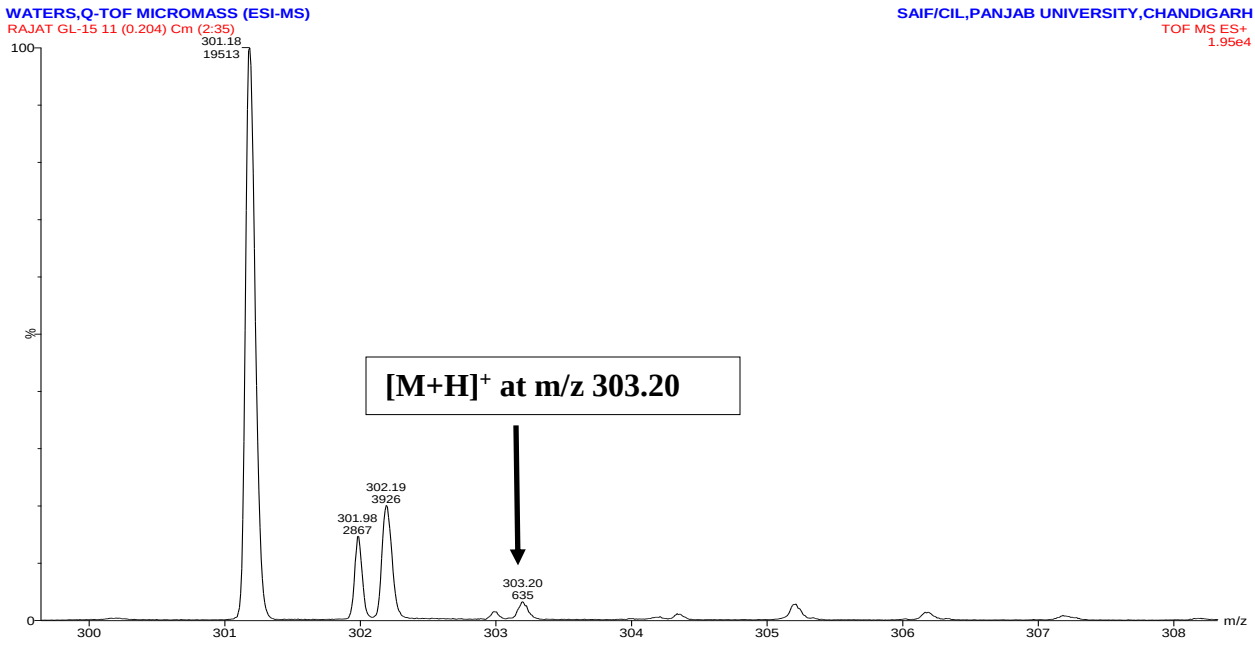

Fig. 27 ESI-MS spectrum of bioactive fraction 3 of GL15 showing m/z value of 303.20

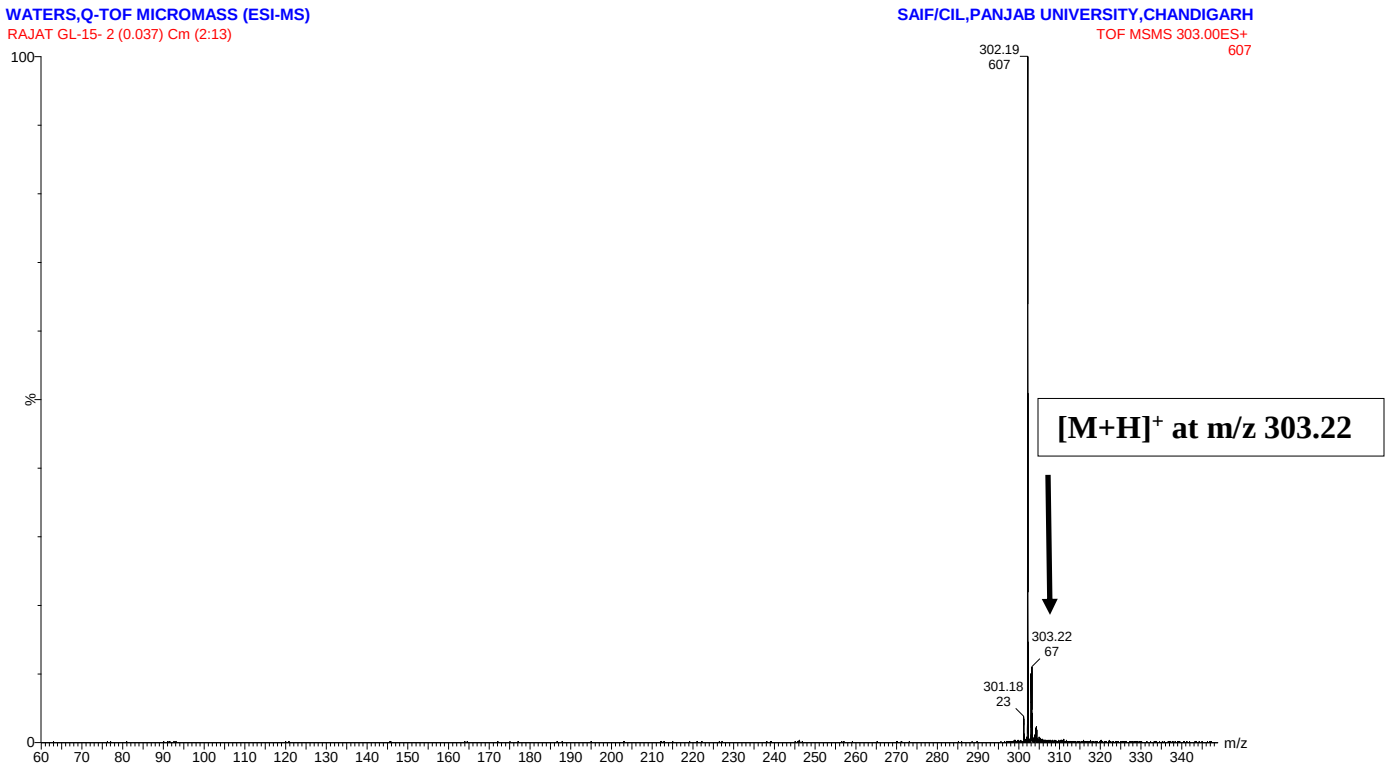

Fig. 28 ESI-MS/MS spectrum of fraction 3 of GL15 showing m/z value of 303.22

4.16. Identification of endophytic fungus GL15 by microscopic and molecular methods

4.16.1. Identification based on morphological characteristics

Endophytic fungus GL15 when grown on surface of PDA plate for 7 days showed that the fungus was white, woolly and floccose and reached 9 cm diameter. On 10th day culture turned grey and on 12th day culture turned black and was sporulating swiftly and profusely. Microscopic analysis of GL15 showed long branched septate hyphae. Spores formed individually on swollen urn-shaped conidiophores and were flattened spherical to egg shaped (Fig. 29). These characteristics were similar to *Nigrospora sp*. The classification of *Nigrospora oryzae* is given in table 10.

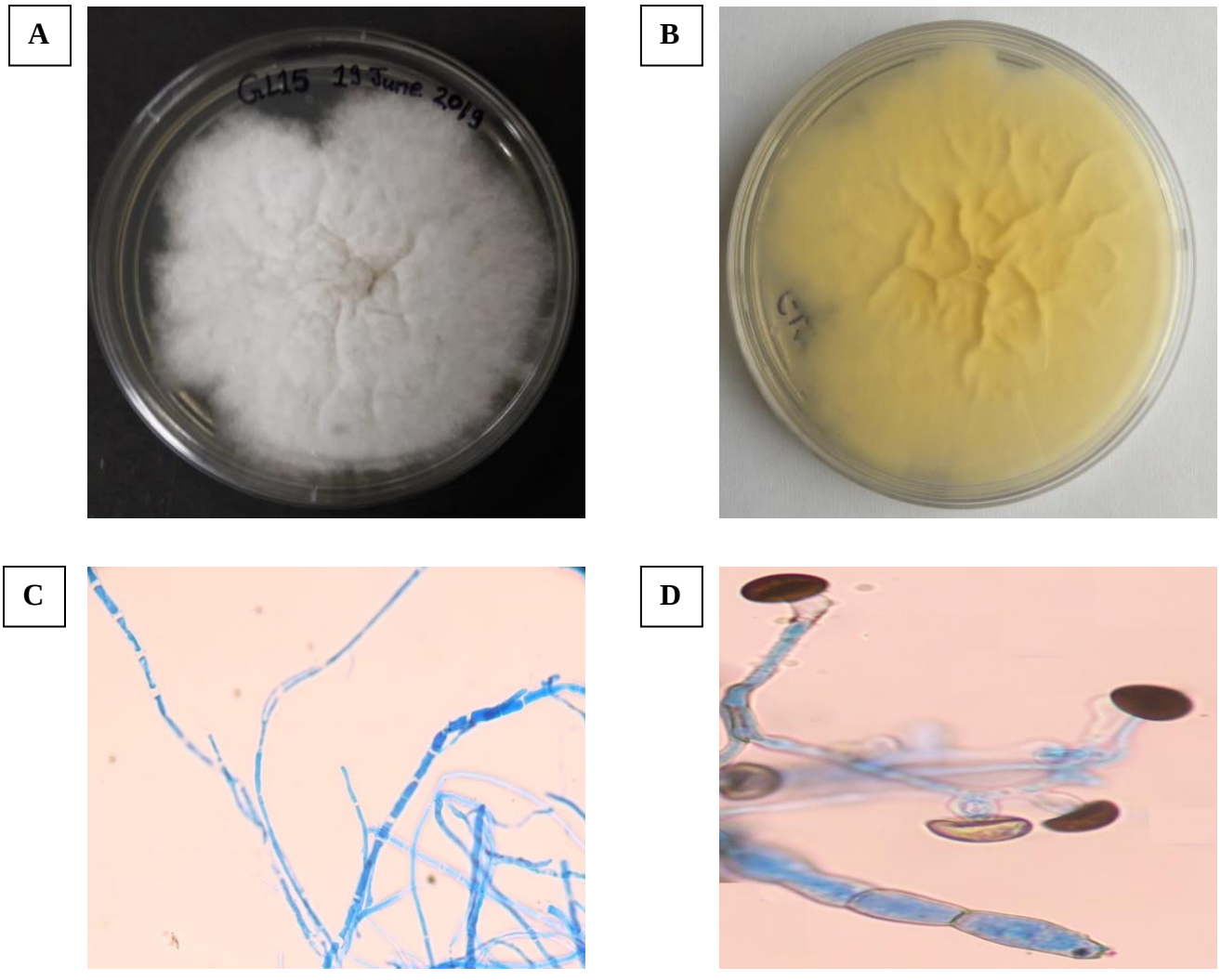

Fig. 29 (A) GL15 on PDA plate-front view (B) GL15 backview (C) Hyphal structure. (D) Conidiophore giving rise to conidia and spores.

Table 10 Classification of *Nigrospora oryzae*

Kingdom	Fungi
Division	Ascomycota
Class	Sordariomycetes
Order	Trichosphaeriales
Genus	*Nigrospora*
Species	*Oryzae*

4.16.2. Molecular based identification of endophytic fungi

Genomic DNA was isolated using CTAB method. The concentration of isolated DNA was found to be 904.9 ng/µl. ITS regions were PCR amplified using forward primer ITS1 and reverse primer ITS4. After purification, PCR product was evaluated by running on electrophoresis gel unit. 1 kb ladder was loaded in lane 2 while amplified PCR products were loaded in lane 3 and 4. (Fig. 30). After confirmation of the PCR product, the concentration was calculated using nanodrop and was found to be 64.1 ng/µl. The A_{260}/A_{280} ratio was 1.82 while the A_{260}/A_{230} ratio was 0.53. The ITS amplified sequence of 504 bp obtained was run through blast n (Fig. 31).

Homologous sequences of different strains were obtained in FASTA format. These sequences were aligned using ClustalW. Evolutionary relationships between homologous sequences were found by neighbor-joining method with a bootstrapping of 1000. MEGA 10 software was used to construct phylogenetic tree (Fig. 32). It confirmed the clustering of GL15 with *Nigrospora. oryzae.*

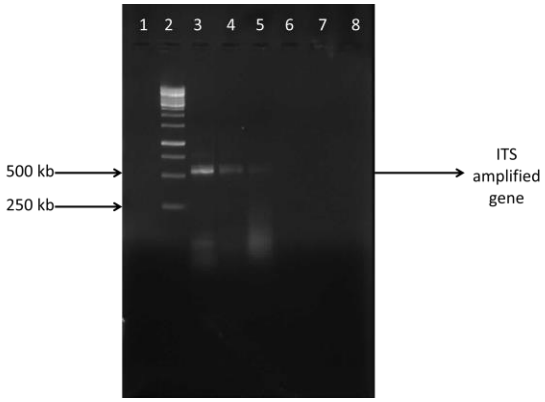

Fig. 30 PCR amplified product of GL15. Lane 2 – 1kb ladder, Lane 3 and 4 – ITS amplified product

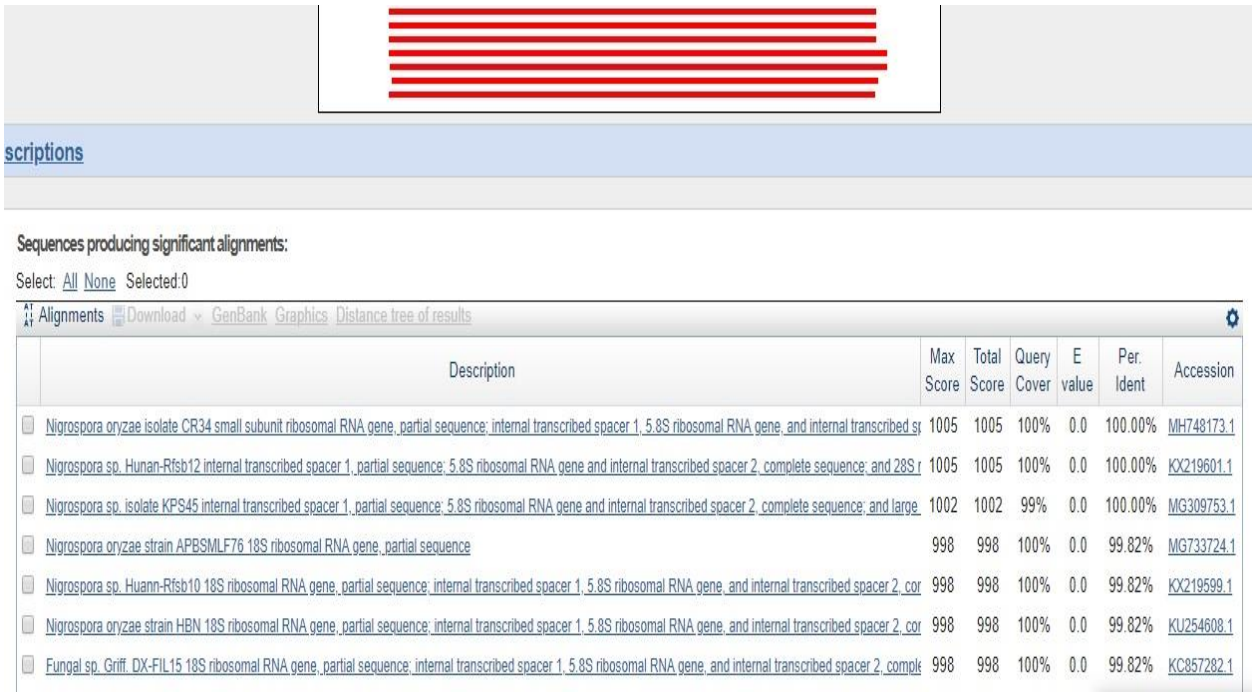

Description	Max Score	Total Score	Query Cover	E value	Per. Ident	Accession
Nigrospora oryzae isolate CR34 small subunit ribosomal RNA gene, partial sequence; internal transcribed spacer 1, 5.8S ribosomal RNA gene, and internal transcribed sp	1005	1005	100%	0.0	100.00%	MH748173.1
Nigrospora sp. Hunan-Rfsb12 internal transcribed spacer 1, partial sequence; 5.8S ribosomal RNA gene and internal transcribed spacer 2, complete sequence; and 28S r	1005	1005	100%	0.0	100.00%	KX219601.1
Nigrospora sp. isolate KPS45 internal transcribed spacer 1, partial sequence; 5.8S ribosomal RNA gene and internal transcribed spacer 2, complete sequence; and large	1002	1002	99%	0.0	100.00%	MG309753.1
Nigrospora oryzae strain APBSMLF76 18S ribosomal RNA gene, partial sequence	998	998	100%	0.0	99.82%	MG733724.1
Nigrospora sp. Huann-Rfsb10 18S ribosomal RNA gene, partial sequence; internal transcribed spacer 1, 5.8S ribosomal RNA gene, and internal transcribed spacer 2, cor	998	998	100%	0.0	99.82%	KX219599.1
Nigrospora oryzae strain HBN 18S ribosomal RNA gene, partial sequence; internal transcribed spacer 1, 5.8S ribosomal RNA gene, and internal transcribed spacer 2, cor	998	998	100%	0.0	99.82%	KU254608.1
Fungal sp. Griff. DX-FIL15 18S ribosomal RNA gene, partial sequence; internal transcribed spacer 1, 5.8S ribosomal RNA gene, and internal transcribed spacer 2, comple	998	998	100%	0.0	99.82%	KC857282.1

Fig. 31 Blast n of amplified sequence of GL15 optimized for homologous sequences.

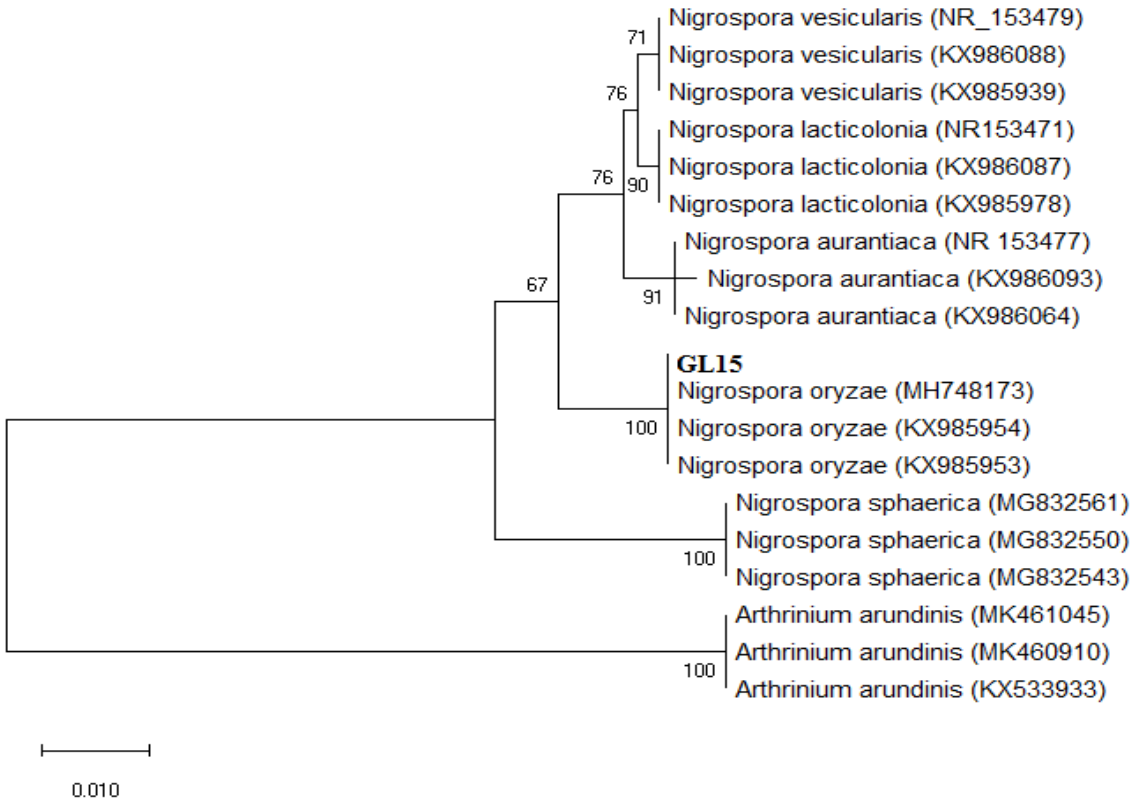

Fig. 32 Neighbor Joining tree showing clustering of ITS amplified sequence GL15 with those of related *Nigrospora sp.* Bootstrap value was 1000.

Chapter 5 Discussion

Endophytic fungi, living asymptomatically can be found within the stems, leaves and roots of plants with wide diversity. Endophytic fungi show mutual relationship with their host plant. They receive nutrition, shelter and protection from the host plant in favor of that host plant may take benefits from enhanced tolerance to biotic and abiotic stress, increased resistance to herbivores, pathogens etc. Large number of metabolites are produced by endophytic fungi that help in promoting the growth of plant. Some of the fungal endophytes, especially those that follow horizontal mode of transmission invade woody plants and show positive impact to host growth and resistance (Saikonnen et al., 1998). Interaction between host plant and endophyte can be affected by various factors such as pattern of infection, conditions of environment, mode of transmission, genetic background (Aly et al., 2011). Medicinal plants have a distinctive invading microbiome that have potential to produce unique and divergent bioactive compounds (Qin et al., 1998). Secondary metabolites holds an stupendous potential for exploring them in medical, agricultural and industrial fields (Zhang et al., 2006).

In the present study, medicinal plant *Tinospora cordifolia* was selected for the isolation of endophytic fungi exhibiting acetylcholinesterase inhibitory activity. The above plant was chosen for study as not much work has been done on the isolation of endophytic fungi and characterization of bioactive compounds. *Tinospora cordifolia* has shown neuroprotective effects in animal model of Parkinson disease (Kosaraju et al., 2014). Therefore, it could be explored for endophytic fungi having capability to produce neuroprotective compounds. A total of 14 endophytic fungi have been isolated from *Tinospora cordifolia*. The isolated fungi were inoculated in the PDB for fermentation. The crude extracts obtained from these isolates were tested for preliminary acetylcholinesterase (AChE) inhibitory and anti-oxidant activities followed by *in vivo* estimations, fractionation, purification and characterization of endophytic crude fungal extract exhibiting acetylcholinesterase inhibitory activity.

During preliminary *in vitro* screening of AChE inhibition out of six fungal extracts GL15-GL20, only GL15 exhibited AChE inhibition which was equivalent to DPZ. GL15 showed highest percentage inhibition of 91.45% at 1 mg/ml. Similarly to our results, 5-methoxy-2-methyl-3-tricosyl-1,4-benzoquinone and 1-O-methylemodin from endophytic fungus *Colletotrichum* of *Huperzia serrat*a have shown significant anti-AChE activity (Li et al., 2018). Further, Long et

al., 2017 reported that austin, dehydroaustinol and preaustinoid isolated from *Aspergillus sp.* exhibited AChE Inhibitory activity with IC50 values of 2.5, 0.40 and 3.00 μM respectively. Azaphilones, armochaetoglobins and xanthenone from endophytic fungus *Chaetomium sp.* showed AChE inhibitory activity with IC_{50} values of 7.34, 5.19, and 4.23 μM respectively (Xu et al., 2017).

In free radical scavenging bioassay, GL17 and GL18 did not show anti-oxidant activity. GL15, GL16, GL19 and GL20 showed maximum anti-oxidant activity at 1000 μg/ml which was comparable to that of ascorbic acid (100 μg/ml). GL15 showed percentage radical scavenging activity of 59.62 at 1 mg/ml. In previous reports, endophytic fungus C*ladosporium. velox* obtained from *Tinospora cordifolia has* shown anti-oxidant activity with IC_{50} value of 22.5μg/mL which was comparable to ascorbic acid (Singh et al., 2016). *Alternaria alternata* an endophytic fungus from medicinal plant, *Azadirachta indica* has shown free radical scavenging activity with IC_{50} value of 38 ± 1.7 μg/mL (Chatterjee et al., 2019).

Cognitive deficits were observed in the SCO-induced animal model (Zaki et al., 2014). Y-maze test is considered as best prototype to measure the cognitive impairments in dementia subjected mice (Krishnamurthy et al., 2013). Moreover, anomalies in cognition are reflected as one of the major symptom of AD (Cai et al., 2018). GL15 (5 mg/kg) and DPZ (3 mg/kg) showed significant attenuation in scopolamine-induced alterations in behavioral contents like novel investigation, spatial recognition memory and coping behavior to novel environment in terms of increase in quantity of arm entries during trial stages, percentage rise in novel arm entries and decrease in anxiety-like behavior respectively in Y-maze paradigm.

Scopolamine is well acknowledged for hampering among the techniques of learning attainment, memory presentation and temporary reminiscence in mice and humans (Shabani et al., 2018). It's dose-vulnerably diminished the latency in the inhibitory escaping assignment and hence it exhibits dementia (Sayyahi et al., 2018). Also, it augmented the appearance of AChE in rats hippocampus (Mushtaq et al., 2018). It straightforwardly caused injury to the hippocampal circuits that might primarily be dependable for learning and memory deficits (Kim et al., 2018).

Passive avoidance test has been broadly authenticated to quantify cognition in mice (Choi et al., 2018). Literature review suggests that PAT could be used to comprehend the natural root of

dementia (Lee et al., 2010). It has been well established that scopolamine modulates process of learning attainment, memory performance and short-term memory in both mice and human beings (Oh et al., 2009). Scopolamine amplifies the concentration of AChE in hippocampus of animals and alterations in amount of AChE might be chiefly responsible for learning and memory impairments (Parent et al., 2004; Kim et al., 2018). Administration of scopolamine showed the decline in latency time in PAT which signifies that scopolamine has induced dementia in experimental animals. Treatment with highest dose of GL15 exhibited the increase in latency period which was comparable with vehicle administered and DPZ subjected mice. However, GL15 when administered at doses of (1.25 and 2.5 mg/kg) did not show any increase in latency period.

The attenuation of cholinergic system has a fundamental function in pathophysiology of cognitive deficit mice (Jahanshahi et al., 2012). Previous reports demonstrate that the turnover of cholinergic activity has been increased due to elevation in the level of AChE in hippocampus (Ferreira-Vieira et al., 2016). Also (Shabani et al., 2018) reported hyperactive hippocampal AChE activity (cholinergic system) in models of dementia. These modulations in the AChE availability may interfere with learning and memory impairments that occur in case of dementia (Rahimzadegan et al., 2018). Hence, it has been illustrated that hyperactive cholinergic system has a central part in dwindling of cognitive impairments. Hence, based upon the above *in vivo* results it show that GL15 exhibits neuroprotective activity via AChE antagonism in dementia subjected mice. GL15 dose-dependently ameliorated the SCO-induced cognitive anomalies in mice. These interpretation highlights the fact that GL15 may mitigate dementia and attenuate the learning and memory anomalies in experimental animals. *In vivo* studies on endophytic fungal extract exhibiting neuroprotective activity have not been reported so far.

UV absorbance spectrum of fraction 3 showed maximum wavelength at 258 nm and 376 nm. The FTIR spectrum of bioactive fraction 3 showed a broad peak in the region of 3410.2 which was due to presence of hydroxyl group. The peak at 1664.2 region is due to presence of carboxyl group. The alkene and ether group were observed at 1610.8 and 1263 respectively (Catauro et al., 2015). ESI-MS analysis of bioactive fraction 3 showed a parent ion of m/z 303.20 (Yu et al., 2019). Quercetin has shown acetylcholinesterase inhibitory activity (Adedara et al., 2017). Quercetin has been isolated from endophytic fungus *Psathyrella condolleana* of medicinal plant,

Ginkgo biloba (Pan et al., 2019). UV absorbance spectrum of quercetin showed maximum wavelength at 258 nm and 372 nm. ESI-MS spectrum of quercetin showed the presence of parent ion at m/z value of 303.10. Based upon the various techniques of characterization, it may be concluded that quercetin is present in fraction 3 of GL15. Microscopic and molecular identification confirmed that GL15 was *Nigrospora oryzae*. Endophytic fungus *Nigrospora sp.* has been isolated from *Tinospora cordfolia* (Thakur et al., 2012). Ebada et al., 2016 reported isolation of quercetin from *Nigrospora oryzae* and its characterization. Quercetin from endophytic fungus, *Nigrospora oryzae* isolated from *Tinospora cordifolia* has not been reported so far.

Chapter 6 Conclusions

In the present study, medicinal plant *Tinospora cordifolia* was selected for the isolation of endophytic fungi exhibiting acetylcholinesterase inhibitory activity. The above plant was chosen for study as not much work has been done on the isolation of endophytic fungi and characterization of bioactive compounds.

In vitro studies on extract GL-15 showed significant anti-oxidant and anti-AChE activities which were analogous to ascorbic acid and DPZ respectively. GL15 showed anti-dementia-like activity in scopolamine model. The minimal effective dose of GL15 modulated the scopolamine-provoked cognitive deficits like impairments in spatial recognition memory and latency period in Y-maze and PAT respectively. GL-15 (5 mg/kg) ameliorated the scopolamine-provoked increase in level of AChE in hippocampus, resulting in dementia. GL15 at highest dose level restored the scopolamine-provoked alteration in cholinergic activity in hippocampus. Consequently, GL15 showed significant decrease in the appearance of AChE. Similarly, DPZ improved the scopolamine-provoked dementia. Column chromatography was run to obtain various fractions of GL15 and fraction 3 of GL15 showed 87.1% percentage AChE inhibition. ESI-MS/MS, FTIR and UV spectroscopic characterizations of bioactive fraction 3 of GL15 show the presence of quercetin which is a potent AChE inhibitor. Molecular and microscopic identification confirmed GL15 to be *Nigrospora oryzae.* These studies indicate that quercetin from endophytic fungus GL-15 may cure the learning and memory shortfalls via AChE mediated mechanism in experimental mice. Hence, it may be concluded that quercetin obtained from endophytic fungus, *Nigrospora oryzae* may play a key role in the management of Alzheimer's disease.

Future scope of work

Neuroprotective compound Quercetin from endophytic fungus, *Nigrospora oryzae* isolated from *Tinospora cordifolia* may exert therapeutic effects against Alzheimer's disease.

References

1. Adedara IA, Ego VC, Subair TI, Oyediran O (2017) Quercetin improves neurobehavioral performance through restoration of brain antioxidant status and acetylchlolinesterase activity in manganese-treated experimental rats. Neurochemical research 42:1219-1229.
2. Al Omairi NE, Al-Brakati AY, Kassab RB, Lokman MS, Elmahallawy EK, Amin HK, Abdel Moneim AE (2019) Soursop fruit extract mitigates scopolamine-induced amnesia and oxidative stress via activating cholinergic and Nrf2/HO-1 pathways. Metab. Brain. Dis. doi:.1007/s11011-019-00407-2.
3. Aly AH, Debbab A, & Proksch P (2011) Fifty years of drug discovery from fungi. Fungal Diversity 50:1-3.
4. Anand P, Singh B, Singh N (2012) A review on coumarins as acetylcholinesterase inhibitors for alzheimer's disease. Bioorg. Med. Chem. 20:1175–1180.
5. Andriana Y, Xuan T, Quy T, Minh T, Van T, Viet T (2019) Antihyperuricemia, antioxidant, and antibacterial activities of *Tridax procumbens L.* Foods doi:10.3390/foods8010021.
6. Ayaz M, Junaid M, Ullah F, Subhan F, Sadiq A, Ali G (2017) Anti-Alzheimer's studies on β-sitosterol isolated from *Polygonum hydropiper L.* Frontiers in pharmacology 8:697.
7. Baskaran R, Priya LB, Sathish Kumar V, Padma VV (2018) *Tinospora cordifolia* extract prevents cadmium-induced oxidative stress and hepatotoxicity in experimental rats. J. Ayurveda Integr. Med. 9:252-257.
8. Beara IN, Torović LD, Pintać DĐ, Majkić TM, Orčić DZ, Mimica-Dukić NM, Lesjak MM (2017) Polyphenolic profile, antioxidant and neuroprotective potency of grape juices and wines from fruška Gora region (Serbia). International journal of food properties 20:2552-2568.
9. Berté TE, Dalmagro AP, Zimath PL, Gonçalves AE, Meyre-Silva C, Bürger C, Weber CJ, Dos Santos DA, Cechinel-Filho V, de Souza MM (2018) Taraxerol as a possible therapeutic agent on memory impairments and Alzheimer's disease: Effects against scopolamine and STZ-induced cognitive dysfunctions. Steroids 132:5-1.
10. Bhattacharjee A, Shashidhara SC, Saha S (2015) Nootropic activity of *crataeva nurvala* buch-ham against scopolamine induced cognitive impairment. EXCLI J. 14:335.10.1719.

11. Bradford M (1976) A rapid and sensitive method for the quantitation of microgram quantities of protein utilizing the principle of protein-dye binding. Anal. Biochem. 72:248-254.
12. Cahlikova L, Opletal L, Kurfurst M, Macakova K, Kulhankova A, Hostalkova A (2010) Acetylcholinesterase and butyrylcholinesterase inhibitory compounds from *Chelidonium sp.* Nat. Prod. Commun. 5:1751-4.
13. Cai P, Fang SQ, Yang HL, Yang XL, Liu QH, Kong LY, Wang XB (2018) Donepezil-butylated hydroxytoluene (BHT) hybrids as Anti-Alzheimer's disease agents with cholinergic, antioxidant and neuroprotective properties. Eur. J. Med. Chem. 157:161-176.
14. Can MV, Tran AH, Pham DM, Dinh BQ, Le QV, Nguyen BV (2018) *Willughbeia cochinchinensis* prevents scopolamine-induced deficits in memory, spatial learning, and object recognition in rodents. J. Ethnopharmacol. 214:99-105.
15. Catauro M, Papale F, Bollino F, Piccolella S, Marciano S, Nocera P, Pacifico S (2015) Silica/quercetin sol–gel hybrids as antioxidant dental implant materials. Science and technology of advanced materials. 16:35-43
16. Chatterjee S, Ghosh R, Mandal NC (2019) Production of bioactive compounds with bactericidal and antioxidant potential by endophytic fungus *Alternaria alternata* AE1 isolated from *Azadirachta indica* A. Juss. PloS one 14(4)e0214744.
17. Choi WY, Kang DH, Lee HY (2018) Effect of fermented *Spirulina maxima* extract on cognitive-enhancing activities in mice with scopolamine-induced dementia. Evid. Based Complement Alternat. Med. doi:10.1155/2018/7218504.
18. Cicero AF, Baggioni A (2016) Berberine and its role in chronic disease. Adv. Exp. Med. Biol. 928:27-45.
19. Dellu F, Mayo W, Cherkaoui J et al (1992) A two-trial memory task with automated recording: study in young and aged rats. Brain Res. 588:132-139.
20. Desai S, Metrani R, Vantamuri S, Ginigeri V, Phadke K, Hungund B (2012) Phytochemical analysis, antimicrobial and antitumour screening of endophytes of *T. cordifolia.* Method1:5-6.
21. Dhama K, Sachan S, Khandia R, Munjal A, Iqbal HMN, Latheef SK (2016) Medicinal and beneficial health applications of *Tinospora cordifolia* (Guduchi): a miraculous herb

countering various diseases/disorders and its immunomodulatory effects. Recent Pat. Endocr. Metab. Immune Drug Discov.10:96–111.

22. Ebada, SS, Eze P, Okoye F B, Esimone C O, & Proksch P (2016) The fungal endophyte *Nigrospora oryzae* produces quercetin monoglycosides previously known only from plants. ChemistrySelect, 1:2767-2771.
23. Ellman GL, K.D. Courtney, V. Andres, R.M. Featherstone (1961) A new and rapid colorimetric determination of acetylcholinesterase activity. Biochem. Pharmacol. doi: 10.12688/f1000research.14506.
24. Ferreira-Vieira, TH Guimaraes, IM Silva (2016) Alzheimer's Disease: targeting the cholinergic System. Current Neuropharmacology 14:510-15.
25. Francis PT, Palmer AM, Snape M, Wilcock GK (1999) The cholinergic hypothesis of Alzheimer's disease: a review of progress. J. Neurol. Neurosurg. Psychiatry. 66:137-47.
26. Gill H, Vasundhara M (2019) Isolation of taxol producing endophytic fungus *Alternaria brassicicola* from non-Taxus medicinal plant *Terminalia arjuna*. World Journal of Microbiology and Biotechnology 35:74.
27. Hadacek F, Greger H (2000) Testing of antifungal natural products: methodologies, comparability of results and assay choice. Phytochemical analysis 11:137-147.
28. Hampel H, Mesulam MM, Cuello AC, Farlow MR, Giacobini E, Grossberg GT (2018) The cholinergic system in the pathophysiology and treatment of Alzheimer's disease. Brain 141:917-1933.
29. Harir M, Bendif H, Yahiaoui M (2019) Evaluation of antimicrobial activity of *Terfezia arenaria* extracts collected from Saharan desert against bacteria and filamentous fungi. 3 Biotech. doi.org/10.1007/s13205-019-1816-3.
30. Jahanshahi M, Azami NS, Nickmahzar EG (2012) Effect of scopolamine-based amnesia on the number of astrocytes in the rat's hippocampus. Int. J. Morphol. 30:388-393.
31. Kapoor N, Saxena S (2018) Endophytic fungi of *Tinospora cordifolia* with anti-gout properties. 3 Biotech. doi.org/10.1007/s13205-018-1290-3.
32. Kharwar RN, Mishra A, Gond SK, Stierle A, Stierle D (2011) Anticancer compounds derived from fungal endophytes: their importance and future challenges. Nat. Prod. Rep. 28:1208–1228.

33. Kim MS, Lee DY, Lee J, Kim HW, Sung SH, Han JS, Jeon WK (2018) *Terminalia chebula* extract prevents scopolamine-induced amnesia via cholinergic modulation and anti-oxidative effects in mice. BMC Complement Altern. Med. doi: 10.1186/s12906-018.
34. Kim SR, Hwang SY, Jang YP, Park MJ, Markelonis GJ, Oh TH, Kim YC (1999) Protopine from *Corydalis ternata* has anticholinesterase and antiamnesic activities. Planta medica 65:218-221.
35. Ko YH, Kwon SH, Lee SY, Jang CG (2017) Liquiritigenin ameliorates memory and cognitive impairment through cholinergic and BDNF pathways in the mouse hippocampus. Arch. Pharm. Res. 40:1209-1217.
36. Kosaraju J, Chinni S, Roy PD, Kannan E, Antony AS, Kumar MN (2014) Neuroprotective effect of *Tinospora cordifolia* ethanol extract on 6-hydroxy dopamine induced parkinsonism. Indian J. Pharmacol. 46:176-80.
37. Krishnamurthy S, Garabadu D, Joy KP (2013) Risperidone ameliorates post-traumatic stress disorder-like symptoms in modified stress re-stress model. Neuropharmacology 75:62-77.
38. Latiffah Zakaria, Wan Nuraini Wan Aziz (2018) Moleculer identification of endophytic fungi from banana leaves (*Musa spp.*) Trop. Life Sci. Res. 29:201–211.
39. Lee B, Park J, Kwon S, Park MW, Oh SM, Yeom MJ, Shim I, Lee HJ, Hahm DH (2010) Effect of wild ginseng on scopolamine-induced acetylcholine depletion in the rat hippocampus. J. Pharm. Pharmacol. 62:263-271.
40. Li Z, Ma N, Zhao PJ (2018) Acetylcholinesterase inhibitory active metabolites from the endophytic fungus *Colletotrichum sp.* YMF432. Nat. Prod. Res. 4:1-4.
41. Lin Z, Wen J, Zhu T, Fang Y, Gu Q, Zhu W (2008) Chrysogenamide A from an endophytic fungus associated with *Cistanche deserticola* and its neuroprotective effect on SH-SY5Y cells. J. Antibiot. 61:81-5.
42. Liu JF, Chen WJ, Xin BR, Lu J (2014) Metabolites of the endophytic fungus *Penicillium sp.* FJ-1 of *Acanthus ilicifolius* Nat. Prod. Commun. 9:799-801.
43. Long Y, Cui H, Liu X, Xiao Z, Wen S, She Z, Huang X (2017) Acetylcholinesterase inhibitory meroterpenoid from a mangrove endophytic fungus *Aspergillus sp.* 16-5c Molecules doi:10.3390/molecules22050727.

44. Mak S, Luk W, W Cui, W Hu, S Tsim, KW Han (2014) Synergistic inhibition on acetylcholinesterase by the combination of berberine and palmatine originally isolated from Chinese medicinal herbs. Journal of molecular neuroscience 53:511-516.
45. Malekiyan R, Abdanipour A, Sohrabi D, Jafari Anarkooli I (2019) Antioxidant and neuroprotective effects of lycopene and insulin in the hippocampus of streptozotocin-induced diabetic rats. Biomed. Rep. 10:47-54.
46. Masuoka T, Uwada J, Kudo M, Yoshiki H, Yamashita Y, Taniguchi T, Nishio M, Ishibashi T, Muramatsu I (2019) Augmentation of endogenous acetylcholine uptake and cholinergic facilitation of hippocampal long-term potentiation by acetylcholinesterase inhibition. Neuroscience 404:39-47.
47. Mishra A, Gond SK, Kumar A, Sharma VK, Verma SK, Kharwar RN, Sieber TN (2012) Season and tissue type affect fungal endophyte communities of the Indian medicinal plant *Tinospora cordifolia* more strongly than geographic location. Microb. Ecol. 64:388-98.
48. Mishra R, Kaur G (2013) Aqueous ethanolic extract of *Tinospora cordifolia* as a potential candidate for differentiation based therapy of glioblastomas. PLoS One. 8(10):e78764.
49. Mishra R, Kaur G (2015) *Tinospora cordifolia* induces differentiation and senescence pathways in neuroblastoma cells. Mol. Neurobiol. 2:719–33.
50. Mushtaq A, Anwar R, Ahmad M (2018) *Lavandula stoechas* (L) very potent antioxidant attenuates dementia in scopolamine-induced memory deficit mice. Front Pharmacol. doi: 10.3389/fphar.2018.01375.
51. Na R, Jiajia L, Dongliang Y, Yingzi P, Juan H, Xiong L, Nana Z, Jing Z, Yitian L (2016) Identification of vincamine indole alkaloids isolated from *Nerium indicum*. Microbiol. Res. 192:114-121.
52. Oh JH, B.J. Choi, M.S. Chang, S.K. Park (2009) *Nelumbo nucifera* semen extract improves memory in rats with scopolamine-induced amnesia through the induction of choline acetyltransferase Neurosci. Lett. 461:41-44.
53. Ohno R, Miyagishi H, Tsuji M, Saito A, Miyagawa K, Kurokawa K, Takeda H (2018) Yokukansan, a traditional japanese herbal medicine, enhances the anxiolytic effect of fluvoxamine and reduces cortical 5-HT_{2A} receptor expression in mice. J. Ethnopharmacol. 216:89-96.

54. Pan Y, Zheng W, Yang, S (2019) Chemical and activity investigation on metabolites produced by an endophytic fungi *Psathyrella candolleana* from the seed of *Ginkgo biloba*. Natural product research 24:1-4.
55. Parent MB, Baxter MG. (2004) Septohippocampal acetylcholine: involved in but not necessary for learning and memory? Learn. Mem. 11:9–20.
56. Pedra NS, Galdino KCA, da Silva DS, Ramos PT, Bona NP, Soares MSP, Azambuja JH, Canuto KM, de Brito ES, Ribeiro PRV, Souza ASQ, Cunico W, Stefanello FM, Spanevello RM, Braganhol E (2018) Endophytic fungus isolated from *Achyrocline satureioides* exhibits selective antiglioma activity-the role of Sch-642305. Front. Oncol. doi: 10.3389/fonc.2018.00476.
57. Pereira DM, Ferreres F, Oliveira JM, Gaspar L, Faria J, Valentão P (2010) Pharmacological effects of *Catharanthus roseus* root alkaloids in AChE inhibition and cholinergic neurotransmission. Phytomedicine 17:646–652.
58. Petrini O, Sieber TN, Toti L, Viret O (1992) Ecology, metabolite production and substrate utilization in endophytic fungi. Nat. Toxin 1:185–196.
59. Pilipenko V, Narbute K, Pupure J, Rumaks J, Jansone B, Klusa V (2019) Neuroprotective action of diazepam at very low and moderate doses in Alzheimer's disease model rats. Neuropharmacology 144:319-326.
60. Qian YX, Kang JC, Luo YK, Zhao JJ, He J, Geng K (2016) A Bilobalide-producing endophytic fungus, *Pestalotiopsis uvicola* from medicinal Plant *Ginkgo biloba.* Curr. Microbiol. 73:280-6.
61. Qin GW, Xu RS (1998) Recent advances on bioactive natural products from Chinese medicinal plants. Medicinal research reviews 18:375-382.
62. Qu Z, Zhang J, Yang H, Gao J, Chen H, Liu C (2017) *Prunella vulgaris L.*, an edible and medicinal plant, attenuates scopolamine-induced memory impairment in rats. J. Agric. Food Chem. 65:291–300.
63. Rahimzadegan M, Soodi M (2018) Comparison of memory impairment and oxidative stress following single or repeated doses administration of scopolamine in rat hippocampus. Basic Clin. Neurosci. 9:5–14.

64. Rajalakshmi M, Anita R (2016) β-Cell regenerative efficacy of a polysaccharide isolated from methanolic extract of *Tinospora cordifolia* stem on streptozotocin-induced diabetic Wistar rats. Chem. Biol. Interact. 243:45–53.
65. Ranganathan N, Mahalingam G (2019) Secondary metabolite as therapeutic agent from endophytic fungi *Alternaria longipes* strain VITN14G of mangrove plant *Avicennia officinalis.* Journal of cellular biochemistry 120:4021-4031.
66. Rawal AK, Muddeshwar MG, Biswas SK (2004) *Rubia cordifolia, Fagonia cretica linn and Tinospora cordifolia* exert neuroprotection by modulating the antioxidant system in rat hippocampal slices subjected to oxygen glucose deprivation. BMC Complement Altern. Med. 13:4-11.
67. Reid SNS, Ryu JK, Kim Y, Jeon BH (2018) GABA-enriched fermented *Laminaria japonica* improves cognitive impairment and neuroplasticity in scopolamine- and ethanol-induced dementia model mice. Nutr. Res. Pract.12:199-207.
68. Saikkonen K, Faeth SH, Helander M, & Sullivan TJ (1998) Fungal endophytes: a continuum of interactions with host plants. Annual review of Ecology and Systematics. 29:319-343.
69. Santos TC, Gomes TM, Pinto BAS, Camara AL, de Andrade Paes AM (2018) Naturally occurring acetylcholinesterase inhibitors and their potential use for Alzheimer's disease therapy. Frontiers in pharmacology 9:15-20.
70. Sayyahi A, Jahanshahi M, Amini H, Sepehri H (2018) Vitamin E can compensate the density of M1 receptors in the hippocampus of scopolamine-treated rats. Folia Neuropathol. 56:215-228.
71. Shabani S, Mirshekar MA (2018) Diosmin is neuroprotective in a rat model of scopolamine-induced cognitive impairment. Biomed. Pharmacother. 108:1376-1383.
72. Sharma A and Kaur G (2018) *Tinospora cordifolia* as a potential neuroregenerative candidate against glutamate induced excitotoxicity: an in vitro perspective. BMC Complement Altern. Med. doi: 10.1186/s12906-018-2330-6.
73. Sheng G, Zhang J, Gao S, Gu Y, Jiang B, Gao Q (2018) SKF83959 has protective effects in the scopolamine model of dementia. Biol. Pharm. Bull. 41:427-434.
74. Singh B, Sharma P, Kumar A, Chadha P, Kaur R, Kaur A (2016) Antioxidant and in vivo genoprotective effects of phenolic compounds identified from an endophytic *Cladosporium*

velox and their relationship with its host plant *Tinospora cordifolia.* J. Ethnopharmacol. 194:450–6.

75. Singh B, Kaur T, Kaur S, Manhas RK, Kaur A (2015) An alpha-glucosidase inhibitor from an endophytic *Cladosporium sp.* with potential as biocontrol agent. Appl. Biochem. Biotechnol. 175:20-34.
76. Singh B, Kaur T, Kaur S, Manhas RK, Kaur A. (2016) Insecticidal potential of an endophyte *Cladosporium volex* against *Spodoptera litura* mediated through inhibition of alpha glycosidases. Pestic. Biochem. Physiol. 131:46-52.
77. Singh SS, Pandey SC, Srivastava S, Gupta VS, Patro B, Ghosh AC (2003) Chemistry and medicinal properties of *Tinospora cordifolia* (Guduchi). Indian J. Pharmacol 35:83–91.
78. Sonaimuthu V, Krishnamoorthy S, Johnpaul M (2010) Taxol producing endophytic fungus *Fusarium culmorum* SVJM072 from medicinal plant of *Tinospora cordifolia*-a first report. Journal of Biotechnology 150:425.
79. Song JH, Lee C, Lee D, Kim S, Bang S, Shin MS, Lee J, Kang KS, Shim SH (2018) Neuroprotective compound from an endophytic fungus, *Colletotrichum sp.* JS-0367. J. Nat. Prod. 81:1411-1416.
80. Squire LR (1992) Memory and the hippocampus: a synthesis from findings with rats, monkeys, and humans. Psychol. Rev. 99:195-231.
81. Stierle A, Strobel G, Stierle D (1993) Taxol and taxane production by *Taxomyces andreanae*, an endophytic fungus of Pacific yew. Science 260:214–216.
82. Sun K, Bai Y, Zhao R, Guo Z, Su X, Li P, Yang P (2019) Neuroprotective effects of matrine on scopolamine-induced amnesia via inhibition of AChE/BuChE and oxidative stress. Metab. Brain Dis. 34:173-181.
83. Tadtong S, Meksuriyen D, Tanasupawat S, Isobe M, Suwanborirux K (2007) Geldanamycin derivatives and neuroprotective effect on cultured P19-derived neurons. Bioorg. Med. Chem. Lett. 17:2939-43.
84. Tamura K, Dudley J, Nei M, Kumar S (2007) MEGA4: molecular evolutionary genetics analysis (MEGA) software version 4.0. Molecular biology and evolution. 24:1596-1599.
85. Tewari D, Stankiewicz AM, Mocan A, Sah AN, Tzvetkov NT, Huminiecki L, Horbańczuk JO, Atanasov AG (2018) Ethnopharmacological approaches for dementia therapy and

significance of natural products and herbal drugs. Front Aging Neurosci. doi: 10.3389/fnagi.2018.00003.

86. Thakur A, Kaur S, Kaur A, Singh V (2012) Detrimental effects of endophytic fungus *Nigrospora sp*. on survival and development of *Spodoptera litura*. Biocontrol science and technology 22:151-161.
87. Uzma F, Narasimha Murthy K, Srinivas C (2016) Optimization of physiological conditions for L-asparaginase production by endophytic fungi (*Fusarium solani*) isolated from *Tinospora cordifolia* (Willd.) Hook. F & Thomson. European Journal of Experimental Biology 6:37-45.
88. Verma VC, Kharwar RN, Strobel GA (2009) Chemical and functional diversity of natural products from plant associated endophytic fungi. Nat. Prod. Communicat. 4:1511–1532.
89. Vinutha B, Prashanth D, Salma K, Sreeja SL, Pratiti D, Padmaja R, Radhika S, Amit A, Venkateshwarlu K, Deepak M (2007) Screening of selected Indian medicinal plants for acetylcholinesterase inhibitory activity. J. Ethnopharmacol. 109:359-63.
90. Wang XC, Xu YM, Li HY, Wu CY, Xu TT, Luo NC, Zhang SJ, Wang Q, Quan SJ (2018) Jiao-Tai-Wan improves cognitive dysfunctions through cholinergic pathway in scopolamine-treated mice. Biomed. Res. Int. doi: 10.1155/2018/3538763.
91. Weller J, Budson A (2018) Current understanding of Alzheimer's disease diagnosis treatment. F1000Res. doi:10.12688.
92. Xiao WJ, Chen HQ, Wang H, Cai CH, Mei WL, Dai HF (2018) New secondary metabolites from the endophytic fungus *Fusarium sp.* isolated from "Qi-Nan" agarwood. Fitoterapia 130:180-83.
93. Xu QL, Xiao YS, Shen Y, Wu HM, Zhang X, Deng XZ, Wang TT, Li W, Tan RX, Jiao RH, Ge HM (2017) Novel chaetospirolactone from an endophytic fungus *Chaetomium sp.* J. Asian Nat. Prod. Res. 20:234-241.
94. Yang Q, Lin J, Zhang H, Liu Y, Kan M, Xiu Z, Chen X, Lan X, Li X, Shi X, Li N, Qu X (2019) Ginsenoside Compound K regulates amyloid β via the Nrf2/Keap1 signaling Pathway in mice with scopolamine hydrobromide-induced memory impairments. J. Mol. Neurosci. 67:62-71.
95. Yang W, Yu J, Zhao L, Ma N, Fang Y, Pei F (2015) Polysaccharides from *Flammulina velutipes* improve scopolamine-induced impairment of learning and memory of rats. Journal of Functional Foods. 18:411–22.

96. Yu W, Wen D, Cai D, Zheng J, Gan H, Jiang F (2019) Simultaneous determination of curcumin, tetrahydrocurcumin, quercetin, and paeoniflorin by UHPLC-MS/MS in rat plasma and its application to a pharmacokinetic study. Journal of pharmaceutical and biomedical analysis. 172:58-66
97. Zaki HF, Abd-El-Fattah MA, Attia AS (2014) Naringenin protects against scopolamine-induced dementia in rats. Bulletin of Faculty of Pharmacy, Cairo University. 52:15-25.
98. Zengin G, Degirmenci NS, Alpsoy L, Aktumsek A (2016) Evaluation of antioxidant, enzyme inhibition, and cytotoxic activity of three anthraquinones (alizarin, purpurin, and quinizarin). Human & experimental toxicology 35:544-553.
99. Zhang HW, Song YC, Tan RX (2006) Biology and chemistry of endophytes. Natural product reports 23:753-771.
100. Zhang L, Seo JH, Li H, Nam G, Yang HO (2018) The phosphodiesterase 5 inhibitor, KJH-1002, reverses a mouse model of amnesia by activating a cGMP/cAMP response element binding protein pathway and decreasing oxidative damage. Br. J. Pharmacol. doi: 10.1111/bph.14377.
101. Zheng XY, Zhang ZJ, Chou GX, Wu T, Cheng XM, Wang CH, Wang ZT (2009) Acetylcholinesterase inhibitive activity-guided isolation of two new alkaloids from seeds of *Peganum nigellastrum* Bunge by an in vitro TLC-bioautographic assay. Archives of pharmacal. research 32:1245-1251.
102. Zhou QY, Yang XQ, Zhang ZX, Wang BY, Hu M, Yang YB, Zhou H, Ding ZT (2018) New azaphilones and tremulane sesquiterpene from endophytic *Nigrospora oryzae* cocultured with *Irpex lacteus*. Fitoterapia 130:26-30.

Appendix

Table 11 PCR reaction mixture composition

Components	**Quantity**
DNA template	1 µl
10X buffer	2.5 µl
Forward primer	1 µl
Reverse primer	1 µl
dNTPSs (2mM)	2 µl
$MgCl_2$ (50mM)	1.5 µl
Nuclease-free water	16 µl
Total Volume	25 µl

Table 12 Composition of PDA

Ingredients	**Gram/liter**
Potato infusion	200
Dextrose	20

Rajat Vig

Title:- Neuroprotective compound Quercetin from endophytic fungus, *Nigrospora oryzae* isolated from *Tinospora cordifolia*

Dissertation

ORIGINALITY REPORT

16%	5%	10%	7%
SIMILARITY INDEX	INTERNET SOURCES	PUBLICATIONS	STUDENT PAPERS

PRIMARY SOURCES

1	Devendra Kumar, Sukesh K. Gupta, Ankit Ganeshpurkar, Gopichand Gutti, Sairam Krishnamurthy, Gyan Modi, Sushil K. Singh. "Development of Piperazinediones as dual inhibitor for treatment of Alzheimer's disease", European Journal of Medicinal Chemistry, 2018 Publication	1%
2	bpspubs.onlinelibrary.wiley.com Internet Source	1%
3	Submitted to Higher Education Commission Pakistan Student Paper	1%
4	Harman Gill, M. Vasundhara. "Isolation of taxol producing endophytic fungus Alternaria brassicicola from non-Taxus medicinal plant Terminalia arjuna", World Journal of Microbiology and Biotechnology, 2019 Publication	1%